EEG-BASED DROWSINESS DETECTION USING SUPPORT VECTOR MACHINE

A Thesis

by

SHAODA YU

Submitted to the Office of Graduate and Professional Studies of
Texas A&M University
in partial fulfillment of the requirements for the degree of

MASTER OF SCIENCE

Chair of Committee,	Peng Li
Co-Chair of Committee,	Seong Gwan Choi
Committee Member,	Yoonsuck Choe
Head of Department,	Chanan Singh

August 2014

Major Subject: Computer Engineering

ABSTRACT

Every year 100,000 car crashes occur as a direct result of driver fatigue resulting in 1,550 deaths, 71,000 injuries, and $12.5 billion in losses as reported by the National Highway Traffic Safety Administration (NHTSA). Another study done by the National Sleep Foundation (NSF) found that drowsiness causes up to 1.9 million crashes a year, with 54% of all drivers having driven while drowsy at least once in the past year, and 28% doing it monthly. It is obvious that drowsiness is a major problem not only from a safety standpoint, but also from a financial one as well. Numerous studies exist in the neuroscience and engineering disciplines that attempt to determine the moment when a person starts to lose focus and drift into sleep. This state change can be detected by various behavioral and physiological measures such as yawning, eye blinking, electroencephalogram (EEG), and electrocardiogram (ECG). There is no general consensus on which of these methods is the most effective and some studies even adopt a hybrid approach in order to maximize the accuracy. The brain's role at the center of the nervous system means it is actively aware of the current cognitive state of an individual, and by measuring the synchronization of neurons fired by various regions of the brain we can acquire a glimpse into this state. Simple events such as eye closures can be easily distinguished from the resulting EEG waveform while more complex mechanisms such as heart abnormalities and sleep stage transitions require a more thorough understanding of the topic in order to develop effective feature extraction and selection methods.

The work presented in this thesis leverages the brain activity collected in the form of electrical currents, known as EEG, with Support Vector Machines (SVM) to

create a classifier which incorporates machine learning that is capable of detecting drowsiness with high accuracy. Traditional drowsiness detection methods utilize the generally defined broadband definitions of the EEG frequency bands in their detection and feature selection algorithms. However, due to the inherently complex nature of EEG signals, particularly with regards to interpersonal differences such as age and health, these drowsiness detection methods for the most part are not able to achieve very good results in terms of accuracy and precision. In addition, recently discovered phenomena point toward unrelated behavior in sub-bands within certain EEG bands, in particular the alpha band which is composed of three sub-bands (one lower and two upper). Contradictory behavior in the lower and first upper alpha band has been observed depending upon the nature and condition of drowsiness. Coupled with the lack of general consensus on the specific sleep stage which encompasses the drowsy state, drowsiness detection becomes a multi-facetted problem which includes many complexities.

Our approach takes advantage of neuroscientific evidence of the awake to sleep transition as a guide for feature selection. To facilitate this process, sub-banding was adopted in order to provide high resolution analysis of the EEG signal as well as flexibility in the selection of frequency ranges for use in the analysis. In addition, techniques to account for interpersonal variability were developed. By selecting a compact set of features that offer the greatest differentiability between the awake and drowsy states, we trained and tested a SVM classifier which provided high performance

with up to 97.94% overall accuracy in classifying between awake and sleep stage 1 during testing.

DEDICATION

Dedicated to my parents, my sister, and Dr. Cyrus Cantrell.

ACKNOWLEDGEMENTS

Thanks to Dr. Li, Dr. Choi, Honghuang Lin, Botang Shao, Qian Wang, and Ehsan Rohani for their contributions and help in this research.

TABLE OF CONTENTS

Page

LIST OF FIGURES

Page

LIST OF TABLES

Page

1. INTRODUCTION

1.1 Motivation

From 18-wheeler truck drivers to airline pilots and traffic controllers to train operators, fatigue is a major concern given the nature of their occupation and the severity of the consequences should they fail to maintain vigilance even for a split second. Electroencephalography (EEG) is the recording of the tiny electrical signals emitted by the brain measuring the activity of millions of neurons. It is most widely used to diagnose disorders such as epilepsy, various sleep disorders, and coma. More recently EEG has been widely utilized for research in the neuroscience and engineering communities for applications such as brain-computer interfaces (BCI) and detection of various disorders. EEG has become popular due to its low cost, non-invasive nature, and reliable means of monitoring human brain activity. EEG is collected using electrodes placed on the scalp. Some systems may require the electrode to make direct contact with the skin which require the user to shave their head, and although inconvenient it provides a cleaner signal. Electrode placement location is specified by the International 10-20 system [18] in order to maintain consistency among different groups.

The transition from wakefulness to sleep is a complex process which is reflected by EEG signal variability within different frequency bands, across the different sleep stages, as well as the nature and origin of the sleep itself. Traditional methods for detecting drowsiness using EEG use a simple threshold to determine the boundary between the two states, but factors like inter-person variability introduce problems and need to be addressed to obtain the correct threshold for each individual [8]. SVM is a

supervised learning algorithm that has also been used previously to classify brain states based on features extracted from an EEG signal [17]. One experiment by Yeo et al that used this method was able to classify between awake and drowsy states with an accuracy of 99.3%. In order to achieve such high accuracy the full set of 19 channels were used along with 4 features across 4 frequency bands, resulting in a 304 feature vector for each epoch of EEG. By carefully selecting features using biomedical studies of the behavior and mechanisms of the brain during the transition from awake to sleep the features that offer the greatest differentiability can be used over the less important features. This will greatly reduce the data processing requirements while still maintaining the high classification accuracy.

Previous studies utilized broadband definitions of the alpha, beta, delta, and theta frequency bands as features without consideration of this complex process, resulting in non-optimal classification accuracy [9] [11].

Our research explores the concept of sub-banding the traditional EEG frequency bands and selecting a core subset for use as features to build a SVM classifier. The selection of the features will be done both manually using neuroscientific studies as well as automatically using a Sparse SVM. We will use publicly available EEG data provided by Physiobank to test and verify the performance of the system.

1.2 Prior work

There have been numerous studies done on using EEG to detect drowsiness. They can be generalized into two classes: threshold based and learning based. This section will cover studies from both classes and focus on the accuracy achieved by each.

1.2.1 Threshold based methods

Park et al put together a one channel EEG device using dry electrodes for signal collection and Matlab for signal processing [11]. These electrodes were placed in the mid-back region of the scalp near the occipital lobe. They computed the total power of the alpha (8-12 Hz), beta (15-20 Hz), and theta (5-7 Hz) EEG bands for each epoch and compared these values to a reference period to determine the changes in power of these bands. The EEG data used was collected and classified by themselves before using the Matlab algorithm to verify the effectiveness of their approach. Various threshold values were tested in order to optimize the algorithm. The experimental data set consisted of 239 total epochs each lasting 1 minute. The highest recall achieved was 86.3% at a threshold level of 0.1%, while the highest precision achieved was 81.3% at a threshold level of 5% [11]. The authors did not mention the precision for the 0.1% threshold nor the recall for the 5% threshold, but it is predicted that with the higher threshold level the algorithm will be less sensitive to changes in the EEG and therefore the recall should be poor. Similarly, at low threshold levels the algorithm is very sensitive to changes and is thus more likely to result in a number of false positives, giving a low precision [11].

In [9] Lin et al used the theta (4-7 Hz) and alpha (8-11 Hz) bands to detect a driver's cognitive state from EEG [9]. They make the assumption that the driver is an alert state during the first few minutes of driving, and thus the first few minutes of EEG recording can be used to derive the driver's alert state. The exact time window of EEG data used to build the alert model was determined by the Mardia test, which means that if the driver is in an alert state then their EEG spectra in the alpha and theta frequency

bands represent a multivariate normal distribution. After the alert model is calculated every epoch of EEG data after the ones used to build the initial alert state is used to measure the deviation from the alert state using Mahalanobis distance. If the driver's EEG spectra in the alpha and theta frequency bands deviate from the alert model then the MD distance will increase, and if it surpasses a set threshold then the system will classify the driver as being drowsy during that time window [9].

The alert model is characterized by a multivariate normal distribution $N(\mu, \sum^2)$, where μ is the mean vector and $\sum$ is the covariance matrix. To compute the deviation of EEG spectra from this model the Mahalanobis distance (MD) is calculated for both the alpha and theta bands. MD provides a relative measure of a given data point's distance from a reference point. Let the alert models of the alpha and theta bands be defined by $N(\mu, \sum^2)_A$ and $N(\mu, \sum^2)_T$ respectively, X_A and X_T be the EEG spectra in the alpha and theta frequency bands respectively, at some time. The MD for the alpha and theta bands can be calculated by the following:

$$\text{MDA}(X_A) = \sqrt{[(X_A - \mu)^T (\sum^2)^{-1} (X_A - \mu)]} \quad (1)$$

$$\text{MDT}(X_T) = \sqrt{[(X_T - \mu)^T (\sum^2)^{-1} (X_T - \mu)]} \quad (2)$$

The MDs above represent the deviation of the EEG spectra during that time interval from the alert state in the alpha and theta bands, respectively. Lin et al combined these two metrics into a single MD by taking a linear combination of MDA and MDT resulting in:

$$\text{MDC} = \alpha \times MDA + (1 - \alpha) \times MDT, \qquad 0 \leq \alpha \leq 1 \quad (3)$$

MDC can be viewed as a combined indicator of drowsiness and the constant α can be tuned to be more sensitive to MDA or MDT, depending on which one experiences a greater change as the driver transitions from an alert state to a drowsy state. A threshold value for MDC is then selected so that if the MDC for a time interval is greater than the threshold, the driver is classified as being drowsy [9].

In order to test their system they designed a virtual reality (VR) based driving experiment where the driver had to try to keep a car centered in a lane. The car was programmed to automatically drift away from the center of the lane in random directions at random intervals to simulate a car drifting on an imperfect road surface. The driver's task was to correct the drift and keep the car in the center of the lane. Three important metrics were recorded during the experiment to determine overall driving performance: deviation onset, response onset, and response offset. Deviation onset is defined as the moment at which the car starts to drift away from the center of the lane. Response onset represents the moment at which the driver begins to correct the drift and response offset is the time that the car returns to the center of the lane. The driver's response time can thus be defined as the duration from deviation onset to response onset. The response time for an alert driver will be much shorter than for a drowsy one so the response time was used directly as a measure of driving performance in the experiment.

To find the optimum threshold value for MDC, F-measure was used. F-measure is the harmonic mean of precision and recall, denoted by

$$F = 2 \times \frac{precision \times recall}{precision + recall} \quad (4)$$

15 subjects' driving performance and MD were analyzed to see the effect on the F-measure by varying the parameter α from 0.1 to 0.9, and the MDC threshold from 1 to 15. Figure 1 shows the resulting average F-measure, precision (also known as PPV), and recall of all the drivers for different MDC thresholds at $\alpha = 0.7$. It can be seen that precision increases as the MDC threshold increases from 7 to 11, and drops sharply after that while recall experiences a steep decline as the MDC threshold increases beyond 7, and the F-measure peaks at an MDC threshold of 7.5 before sharply dropping off beyond that. Intuitively this means that while a small MDC threshold value results in a system that is very sensitive to changes in the MDC and can give a high overall drowsiness detection rate, it is at the same time more likely to wrongly classify a subject as being drowsy when he/she is in fact alert. The results of the optimal F-measure test described above are listed in Table 1. The maximum F-measure obtained was 77.6% (69.2% precision and 88.3% recall) with $\alpha = 0.9$ and $MDC_{Threshold} = 7.5$ [9].

Using the optimal value of α and $MDC_{Threshold}$ determined by the F-measure test above, ten subjects performed the driving performance exercise to test the accuracy of the system. The results are listed in Table 2. The average F-measure of all 10 subjects is 82% (76.9% precision and 88.7% recall). It is important to note that the system's performance was very poor for 2 of the subjects (subject 2 and 9) comparatively, with F-measure values well below the average. This is most likely due to inter-person variability in EEG between individuals, and represents one of the problems with using a strictly defined threshold for drowsiness detection.

1.2.2 SVM based methods

Taking a different approach from threshold based methods, Yeo et al describes an automatic method to detect drowsiness onset while driving using SVM in [17]. This study differs from the others in that they acknowledge that sleep onset during driving differs from normal sleep studies, where subjects actively resist falling asleep and try to maintain vigilance in the former while in the latter subjects are free to fall asleep.

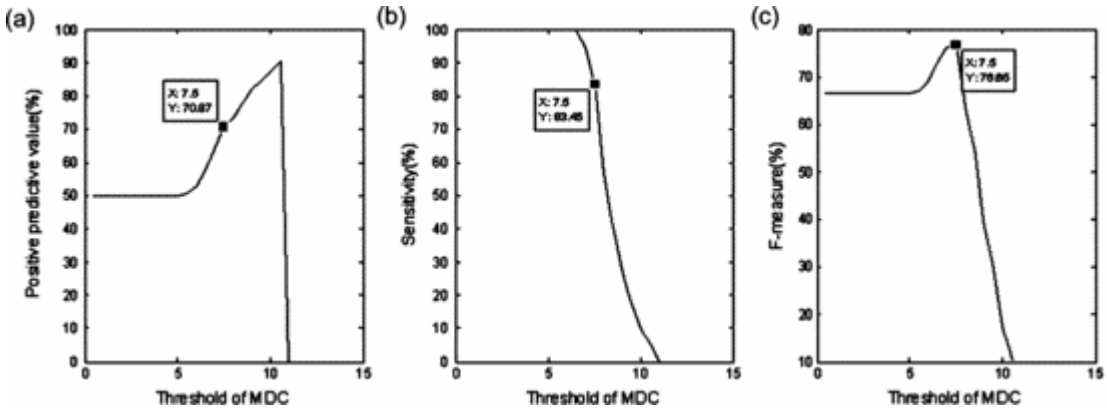

Figure 1. Result of (a) Precision (PPV), (b) sensitivity, and (c) F-measure of 15 subjects corresponding to different thresholds at α = 0.7. Reprinted with permission from [9]. © 2010 IEEE.

Types	Optimal F-measure (%)	Threshold	PPV (%)	Sensitivity (%)
MDT	73.9	6.5	60.2	95.9
MDA	77.3	7.5	69.7	86.9
MDC ($\alpha = 0.1$)	73.5	6.5	59.3	96.6
MDC ($\alpha = 0.2$)	73.8	6.5	58.9	98.6
MDC ($\alpha = 0.3$)	74	7	63.7	88.3
MDC ($\alpha = 0.4$)	75.1	7	63.9	91
MDC ($\alpha = 0.5$)	76.0	7	63.9	93.8
MDC ($\alpha = 0.6$)	76.3	7	64.3	93.8
MDC ($\alpha = 0.7$)	76.7	7.5	70.9	83.5
MDC ($\alpha = 0.8$)	77.4	7.5	70.7	85.5
MDC ($\alpha = 0.9$)	77.6	7.5	69.2	88.3

Table 1. Optimal F-measure results under different conditions. Reprinted with permission from [9]. © 2010 IEEE.

Subject	F-measure (%)	PPV (%)	Sensitivity (%)
1	77.7	75.5	80
2	72.2	78.8	66.7
3	89.1	80.4	100
4	87.5	77.8	100
5	87.4	77.6	100
6	88.9	80	100
7	83.5	78.7	88.9
8	81.1	77.9	84.6
9	66.1	65.5	66.7
10	86.8	76.6	100
Average	82	76.9	88.7

Table 2. Results of the drowsiness detection test. Reprinted with permission from [9] © 2010 IEEE

EEG recording was done using a 32 channel Medtronic PL-Windsor system with a sampling frequency of 256 Hz and a cutoff frequency of 35 Hz. Full head mapping was done using the international 10-20 system of electrode placement. The driving experiment consisted of simulated driving on a straight highway mostly free of other vehicles to produce a monotonous environment where it's easy to fall asleep. 20 subjects performed the experiment for an hour each. Epochs of raw EEG data containing movement artifacts were removed by visual inspection and excluded from the study. The EEG data was manually classified as either "alert" or "drowsy" by two authors trained in interpreting the EEG in 10 second epochs. Eye blink data was used in combination with the raw EEG to help in manual classification [17].

To be classified as "alert" the subject's had to exhibit activity in the beta (13-25 Hz) frequency band while the eye blinks have 0.3-0.4 sec duration with 6-8 sec blink intervals. A drowsy epoch on the other hand was characterized by the appearance of alpha dropouts, eye blink duration greater than 0.5 sec, and more than 50% of EEG data showing alpha activity. The two raters classified the EEG data for every 10 sec epoch independently and then discarded the epochs where there was disagreement. The resulting manually classified epochs were then divided evenly into two sets, one for training and another for testing, with each set containing a mixture of alert and drowsy epochs [17].

Feature extraction and selection is then needed to retrieve a set of features from the raw EEG that can offer good distinguishability between alert and drowsy EEG. The features used were based on the power spectrum of each 10 sec EEG epoch. A Fast

Fourier Transform (FFT) was performed on each epoch using a Hanning window with 256 points and 50% overlap. This was done for all the channels. The power spectrum density function was then calculated and divided into four standard EEG frequency bands relevant to the study of sleep onset: delta (0.5-4 Hz), theta (4-8 Hz), alpha (8-13Hz), and beta (13-20 Hz). The following four features were then extracted from each frequency band [17]:

1. Dominant frequency – From the PSD of a given frequency band the peaks were identified and two frequencies relative to the peak were identified; one on the rising edge and the other on the falling each. These two frequencies each have half the power of the peak they encompass, and the frequency zone in between is defined as the full width half maximum band of the peak. Of all the peaks in a given frequency band, the one with the greatest average power in its full width half maximum band represents the dominant peak, and its corresponding frequency is the dominant frequency. The dominant frequency essentially represents the frequency zone containing the most bandwidth within a given frequency band.
2. Average power of dominant peak – Defined as the average power of the full width half maximum band of the dominant peak mentioned above, it represented the significance of the dominant peak.
3. Center of gravity frequency (CGF) – Defined as $CGF = \frac{\sum_i P(fi) \times fi}{\sum_i P(fi)}$, the CGF is the average of frequency f_i over the frequency domain, weighted by the

power spectrum density $P(f_i)$. This feature is a measure of how high the frequencies in a spectrum are on average.

4. Frequency variability – This feature measures the spread of the frequencies in a given frequency band. It is given by $FV = \frac{\sum_i P(fi)\times fi^2 - [\sum_i P(fi)\times fi]^2 / \sum_i P(fi)}{\sum_i P(fi)}$

After these 4 features were extracted for each of the 4 frequency bands in a 10 sec epoch of EEG data in each of the 19 channels, they ended up with a 304 feature vector for each epoch ($4\ features\ x\ 4\ bands\ x\ 19\ channels$).

Twenty healthy subjects between the ages of 20 and 25 were chosen to participate in the one hour long simulated driving task, in which they attempted to maintain vigilance as much as possible. A breakdown of the EEG data collected during the experiment from all subjects revealed that all subjects fell into stage 1 sleep, with some even falling into deep sleep. Specifically, alert epochs consisted of 8% of the total experiment time while drowsy epochs accounted for 22% of the total time.

The remainder of the time comprised of epochs where the subject had dosed off into deeper levels of drowsiness or had fallen asleep altogether past sleep stage 1. Figure 2 shows an example of a manually scored EEG for a 1 hour driving task used by subjects in this study. Note that the subject experienced multiple episodes of drifting into drowsiness and sleep through the 1 hour interval as he/she struggled to remain alert.

A SVM classifier was trained using the training set and consequently tested for its accuracy in distinguishing between alert and drowsy states using the testing set. The total set of alert and drowsy EEG epochs contained 478 alert epochs and 1404 drowsy epochs, respectively. The training and testing sets contained 239 alert epochs and 702

drowsy epochs each. There were 58 ambiguous epochs which the two raters did not agree on and therefore excluded from the study, showing that raw EEG analysis can be a complicated process. The accuracy achieved on the testing set was 99.3%, showing that the SVM classifier performed very well.

Although the feature selection used to train the SVM classifier resulted in very high accuracy there are some issues that were not addressed in the study. Firstly, there was no consistency in the manual classification process, where only EEG epochs agreed by both raters to be alert or drowsy were included for the study and ambiguous epochs were excluded. By selectively including certain data and discarding others they have artificially increased the accuracy of their SVM classifier, and in real world applications there will undoubtedly be cases where the EEG will contain a lot of noise and be hard to distinguish. Secondly, the subjects used for the experiment represented only a small portion of the general population with a narrow age range and no health problems. This ensured that there were minimal inter-person differences among the subjects. It would be good to test the accuracy of the classifier on a more varied population sample with a wider age range, various health problems, and different sleep schedules. Thirdly, the study utilized EEG recordings from the full 19 channels to achieve such high accuracy levels, but realistically using all 19 channels may not be feasible in real world applications due to the high cost as well as being uncomfortable to wear. Therefore it is important to minimize the number of channels, and therefore features, needed while maintaining the high classification accuracy.

Figure 2. Alert, drowsy, and sleep episodes as scored by EEG manually from a typical 1-h driving simulation. Reprinted with permission from [17].

2. ELECTRODE PLACEMENT

2.1 The international 10-20 system

The now widely used 10-20 standard for electrode placement had its roots at the first International EEG Congress held in London in 1947, where Dr. Herbert Jasper was tasked with coming up with methods to standardize the placement of electrodes for EEG recording. At that time the electrode placement systems used at various research centers were similar, but each had their own convention of designations, resulting in completely different letters and numbers. The following guidelines were established as goals of the new standard [18]:

1. The positioning of electrodes should be based on specific measurements of standard human skull landmarks, and the measurements should be proportional to both the size and the shape of the skull.
2. The new standard for electrode placement should provide adequate coverage of all parts of the skull.
3. Electrode designations should be expressed in terms of brain areas covered in order to provide meaningful information.
4. Anatomical studies should be performed in order to provide additional documentation correlating electrode placement with cortical areas they originated from.

The measurement technique is based on standard features of the human skull, Figure 3 depicts a graphical overview of a human skull with important features labeled. The first measurement is taken from the nasion (front of skull) to the inion (back of

skull) in the anterior-posterior plane. This measurement was then divided into 5 different regions. The first region extends from the nasion for 10% of the total measurement distance towards the inion, this section is labeled Fp (frontal polar). The second, third, and fourth sections are placed successively after Fp, with each section covering 20% of the total measurement distance, these sections are denoted F (Frontal), C (Central), and P (Parietal). The remaining 10% ending at the inion is labeled O (occipital). Figure 4 displays the 5 labeled areas and the corresponding line of electrodes from a side view of the skull. Lateral measurement from the left preauricular point near the ear to the right preauricular point were made. The area can again be divided into 5 sections. Two regions encompassing 10% of the total measurement distance each were located above the two preaurecular points near the ears and labeled as T for temporal.

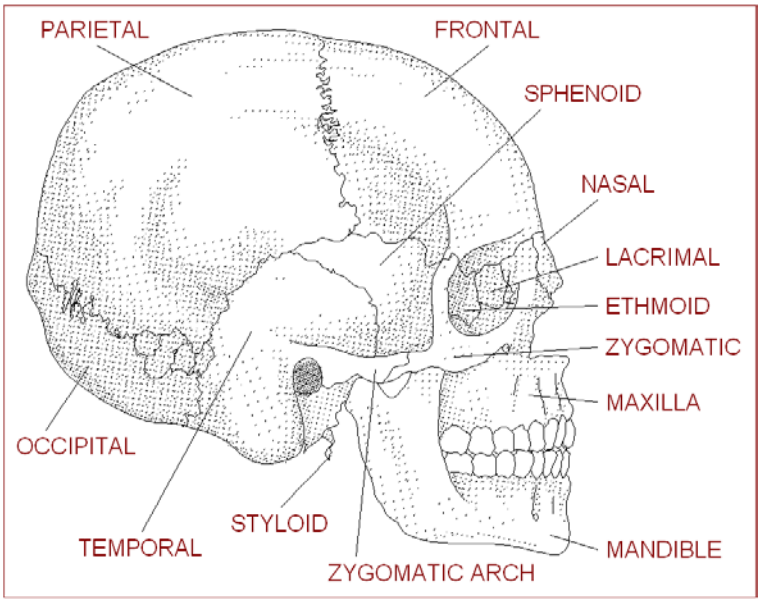

Figure 3. Human skull anatomy

From the two T points, successive marks were made at 20% of the total measurement, meeting at the central location on top of the skull. These two points are labeled left and right C, respectively. Figure 5 provides a graphical overview of this measurement from a frontal view. Next a circumferential measurement over the temporal lobes is taken from the center frontal polar to the center occipital positions. Following the previous measurements, the area is divided into 5 sections the first covering 10% of the total measurement, followed by four sections covering 20% each, and 10% in the last section. The sections are labeled Fp1/Fp2 (left or right Fp), F7/F8 (inferior frontal), T3/T4 (mid temporal), T5/T6 (posterior temporal), and O1/O2 (left or right occipital) respectively (Figure 6) [18]. Anterior-posterior measurements taken from the left and right front parietal positions through the lateral central position to the left and right occipital positions.

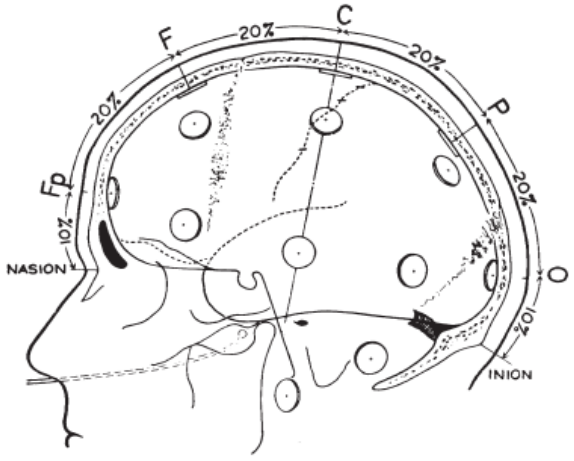

Figure 4. Lateral view of skull. Reprinted with permission from [22].

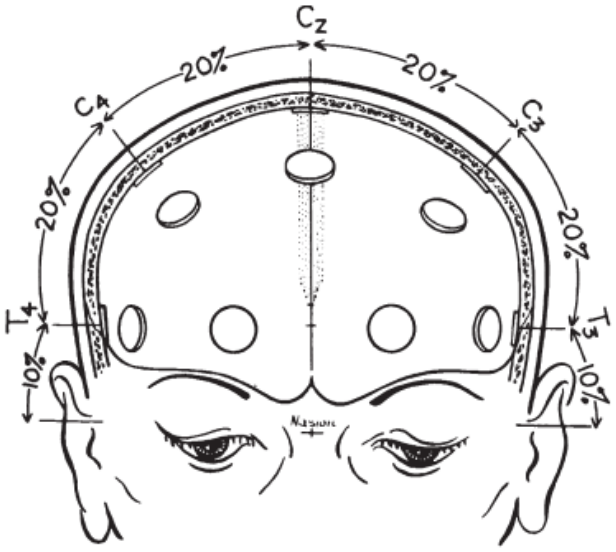

Figure 5. Frontal view of the skull. Reprinted with permission from [22].

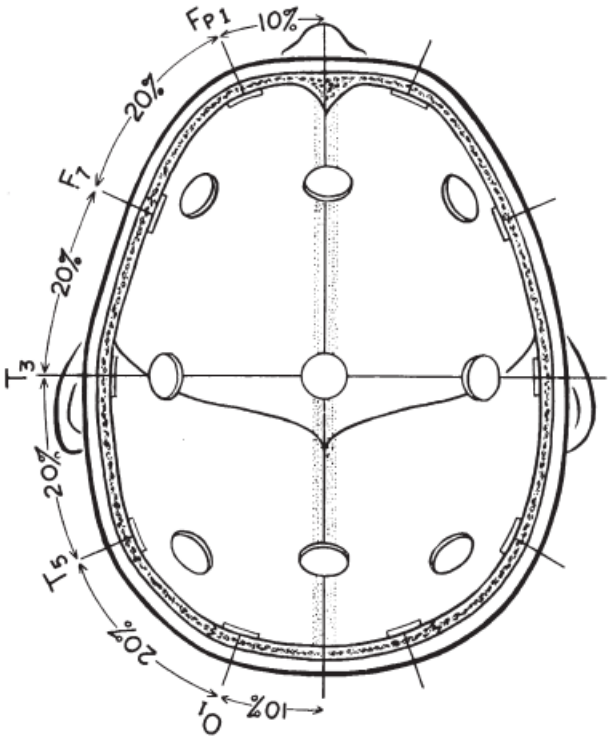

Figure 6. Superior view of the skull. Reprinted with permission from [22].

The area spanning this measurement was divided into equal regions each comprising 25% of the total measurement, these are labeled lateral F, lateral C, and lateral P respectively. Anterior coronal measurements taken from the left and right inferior frontal positions through the center frontal position were divided into equal 25% segments and represents the left lateral frontal, front vertex, and left lateral frontal. Similarly a posterior coronal measurement was taken from the left posterior temporal through the center parietal and divided into 25% sections denoted as left lateral P, P, and right lateral P respectively. Figure 7 provides a graphical illustration [18].

The 19 out of the 21 total electrode placements covered up to this point make up the majority of the 10-20 system (Figure 8). The remaining two electrodes are placed on the ear lobes and labeled as A1/A2 (auricular). The electrode placement labels correspond with anatomical terms for the cortical areas recorded.

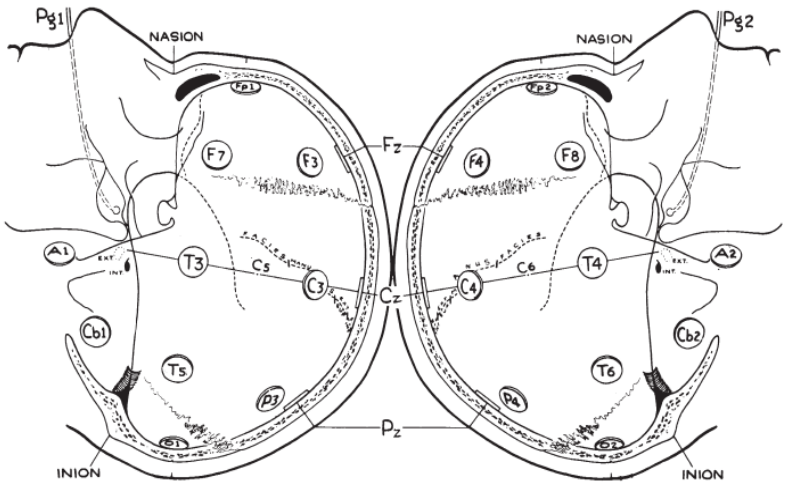

Figure 7. Lateral view of the left and right hemispheres of the skull. Reprinted with permission from [22].

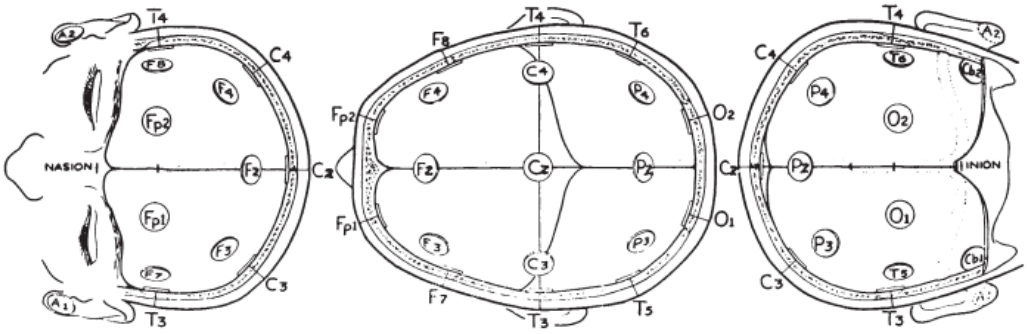

Figure 8. Frontal superior and posterior views showing all the standard electrode positions. Reprinted with permission from [22].

The numbers after the letters serve to differentiate between the left and right homologous regions, with the left side indicated by odd numbers and right side by even numbers. The labels with the letter z in place of a number (Fz, Cz, and Pz) were originally labeled F0, C0, and P0 respectively, but changed later with z for zero. The numbering system allows for additional electrodes to be placed with consistent labels, for example F2 between Fz and F4, or F6 between F4 and F8. The final placements and labels of electrodes using the 10-20 system is shown in figure 9 [18].

Anatomical studies were performed on the heads of cadavers to determine the cortical areas covered by the electrodes in the 10-20 system. Electrodes were placed on the head according to the 10-20 system after measurements were taken. The underlying cortex of the brain were marked using India ink after drilling holes at the marked electrode positions. India ink is a simple black ink that is commonly used in medical applications due to its durability when submerged in preservative fluids and resistance to tissue processing methods.

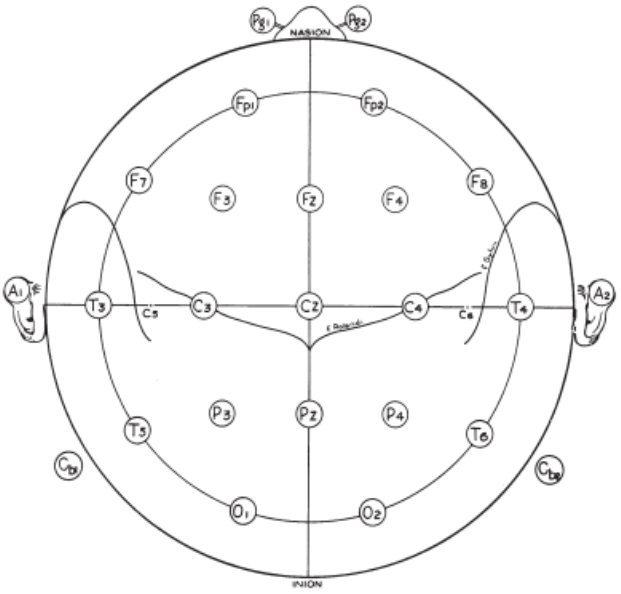

Figure 9. Diagram showing the locations of all the standard electrode positions. Reprinted with permission from [22].

Examination of the brain after removal concluded that despite some variability, the locations of the principle central and sylvian fissures, were within 1 cm of the marks shown in figure 9 [18].

3. NEUROSCIENTIFIC STUDIES ON THE ONSET OF SLEEP

Numerous studies and experiments in the neuroscience and biomedical communities have shown that the human brain is extremely complex and care must be taken in analyzing EEG data. EEG behavior is dependent on various factors such as inter-person differences, definition of sleep stages, definition of the common frequency bands, and the nature of drowsiness. This section will provide a thorough overview of EEG related to drowsiness as well as cover the various phenomena mentioned above. In order to build an effective system for drowsiness detection using EEG, one must have a deep understanding of the fundamental underlying physiological changes accompanying the EEG signals.

3.1 Stages of sleep

The different stages of sleep were first described by Alfred Lee Loomis et al in 1937, when they separated sleep into 5 stages (A to E), which represented the entire spectrum from awake to deep sleep, based on the different EEG features observed [20]. Later on Rapid Eye Movement (REM) sleep was discovered and considered to be distinct from the other stages in 1953 [21]. Consequently, Dement and Kleitman reclassified the sleep stages into 4 Non-REM (NREM) and REM [21]. Finally, in 1968 Rechtschaffen and Kales published “A Manual of Standardized Terminology, Techniques, and Scoring System for Sleep Stages of Human Subject” [13], which has since gone on to become the standard manual used to score sleep stages. According to the Rechtschaffen and Kales standard, sleep can be classified into 5 stages, comprised of 4 NREM and 1 REM stage.

The behavioral and physiological indicators of the different stages are as follows:

Stage 0 – Subject is awake and alert.

Stage 1 – This is the beginning of the sleep cycle and traditionally considered as the transition between wakefulness and sleep, also known as the drowsiness stage. This stage typically lasts 5-10 minutes and the eyes are normally closed, however if awakened from this stage the person may not feel like they slept. In EEG this stage is characterized by high amplitude alpha and theta waves, which are low frequency waves.

Stage 2 – During this stage body temperature begins to drop and the heart rate starts to slow as the body prepares for deep sleep. Lasting for around 20 minutes, in this stage the brain begins to produce short bursts of rapid, rhythmic brain wave activity in the 12-14 Hz range known as sleep spindles. Sleep spindles are usually preceded by K-complexes, which consists of a brief positive voltage peak and transition into a negative voltage peak. K-complexes are comprised of 0-4 Hz waves. Figure 10 illustrates these phenomena. Studies suggest sleep spindles and K-complexes are the results of the brain's attempt to keep the person in a tranquil state to protect sleep as well as engage in memory processing. Along with sleep spindles, K-complexes are defining characteristics of the onset of stage 2 sleep.

Stage 3 – Commonly viewed as a transition between light and deep sleep, in this stage people become less responsive and are generally not aware of external

noises and surroundings. This stage is characterized by the emergence of delta waves in the 0-4 Hz range.

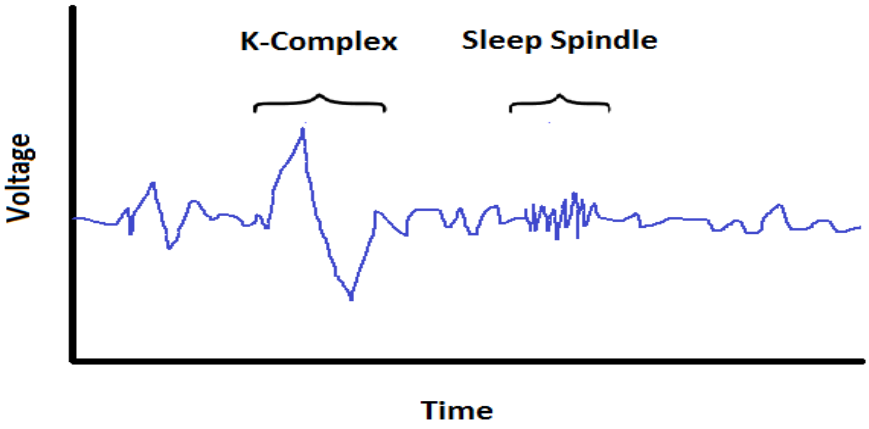

Figure 10. K-complex followed by a sleep spindle.

Stage 4 – Commonly referred to as delta sleep due to the delta waves that occur during this stage. This is the last stage NREM sleep stage that normally lasts around 30 minutes. Phenomena such as sleep walking and bed wetting are most likely to occur at the end of this stage.

Stage 5 – Also known as REM (Rapid Eye Movement) sleep, this stage is characterized by eye movements and increased brain activity. Heart and respiration rates also increase and become erratic. Most memorable dreams occur in this stage as a result of the increased brain activity. As a built-in protection, all voluntary muscles such as the legs and arms are immobilized to prevent one from acting out his/her dreams, involuntary muscles such as the heart and lungs

continue to function as normal. REM sleep is also commonly known as paradoxical sleep due to the increased eye movement and brain activity but paralyzing effect on voluntary muscles.

Despite appearing as a progressive sequence from light drowsiness to deep REM sleep, actual sleep of healthy humans do not follow these stages in sequence. Sleep begins in stage 1, then progresses through stages 2, 3, and 4 as expected. At this point however stage 3 is repeated again before entering REM sleep. After REM sleep the body returns to stage 2, this completes one cycle, of which a healthy person will usually experience 4-5 throughout a night of sleep [13]. A hypnogram depicting the progression through the sleep stages for a healthy adult during a normal night of sleep is displayed in Figure 11.

The sleep cycle mentioned above can be affected by several factors such as sleep disorders, sleep deprivation, changing sleep schedule, stress, and the environment. These variables can shorten or increase the duration of certain sleep stages as well as affect the time it takes to progress to the next sleep stage. Age also plays an important role in this process.

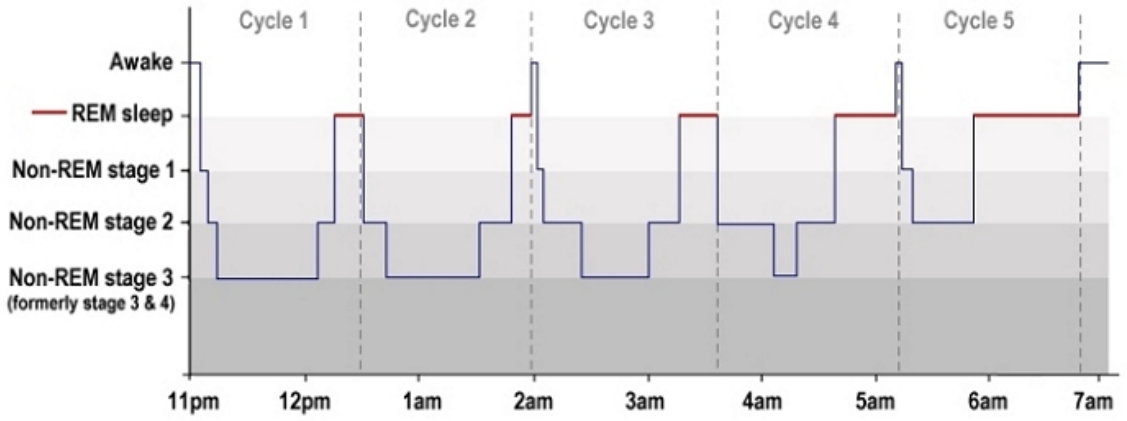

Figure 11. Typical sleep cycle.

Infants and children experience the highest percentage of REM sleep overall, whereas for teens and young adults the percentage drops slightly, and continues to decline further with old age [13]. This is why older people don't need as much sleep compared to before.

3.2 Quantitative EEG changes during sleep onset

Since there is no general consensus on whether the beginning of stage 1 or 2 sleep should be used to define the onset of sleep, it is important to study the quantitative EEG characteristics between awake and the two sleep stages to gain an understanding of the microstructural changes of EEG powers during sleep onset. A study by Gennaro et al examined the changes in EEG powers during the wakefulness-sleep transition by analyzing changes in sub-band single Hz resolution as well as broadband frequency bands [4]. The study collected EEG recordings from twenty six healthy male subjects with normal sleep schedules.

Each subject slept for at least two consecutive nights in a controlled environment starting at 11:30pm and lasting 7.5 hours. The first night's sleep is meant for adaptation to the environment. The recording device was an Esaote Biomedica VEGA 24 with seven unipolar EEG channels (C3-A2, C4-A1, Fpz-A1, Fz-A1, Cz-A1, Pz-A1, Oz-A1) placed according to the standard international 10-20 system. The EEG signals were low pass filtered at 30 Hz. EOG and EMG were also recorded to supplement the EEG recordings [4].

Only sleep data from the second night and onwards were used in this study as the first night was purely meant for the subject to adapt to the environment so there would be no adverse effects. The recordings were manually scored according to the sleep stages defined by the Rechtschaffen and Kales standard in 12 sec epochs. The wakefulness-sleep transition is dependent upon inter-person variables that affect the duration of the transition as well as discontinuity in the process reflected by an alternating pattern of awake and stage 1. To account for these variables and ensure that individual transitions are comparable Gennaro et al combined individual 12 sec epochs into 6 and 10 minute intervals, for spectral EEG analysis when stage 1 and 2 sleep are used to define sleep onset, respectively. For the stage 1 case, 3 minutes of EEG recordings before and 3 minutes after were combined, similarly for the stage 2 case, 5 minutes of EEG recordings before and 5 minutes after were combined for spectral analysis. The discrepancy between the time intervals used for spectral analysis is attributed to specific characteristics of the wakefulness-sleep transition. In a relaxed awake state before sleep, muscular and ocular artifacts occur at a higher rate as a function of the distance from

onset of stage 1 sleep due to increased movement and eye blinks. A shorter interval was therefore chosen for the stage 1 case to minimize artifacts as well as average comparable physiological states [4].

EEG recordings from the C3-A2 channel underwent manual artifact removal based on visual inspection before FFT was performed using a 4 sec resolution, with three consecutive 4 sec epochs averaged together to align with the manually scored 12 sec epochs. Power values were calculated in 0.25 Hz resolution across the 1-28 Hz frequency range, then averaged over adjacent frequencies to obtain power values for 1 Hz resolution bins. For example, the 1 Hz bin contains the averaged absolute power values of the 1-1.25, 1.25-1.5, and 1.5-1.75 Hz frequencies. The power values across individual subjects were aligned to the respective first epoch of stage 1 or stage 2 sleep.

Figure 12A plots the log transformed power values for all 1 Hz bins from 1-28 Hz during the 3 minutes before and after of the first stage 1 epoch averaged across the 26 subjects. The averaged power values were fitted with the best fitting slope for each frequency, and the vertical line in the middle represents the onset of stage 1 sleep. Different colors grouped the individual frequencies into their respective traditional EEG bands. The average power in the 1-6 Hz frequency range increased during the transition to stage 1 sleep onset. EEG power for 7-8 Hz did not display any systematic changes leading up to the stage 1 transition. EEG power in the 9-12 Hz range decreased during the transition while power within 13-15 Hz did not show any systematic changes. The power within the 16-28 Hz decreased during the entire transition period [4].

Figure 12B plots the log transformed power values for all 1 Hz bins from 1-28 Hz during the 5 minutes before and after the first stage 2 epoch averaged across all subjects. Here it can be observed that power in the 1-7 Hz range increased steadily leading up to the stage 2 onset point, at which time the power values experienced a steep increase before levelling off. The 8-12 Hz range showed a steady decrease in power up until the first epoch of the stage 2 transition and subsequently decreased afterwards [4].

The 12-15 Hz range held steady with little to no change until the stage 2 transition, at which time a sudden increase in power is observed. No changes were observable in the 16-17 Hz range while the 18-28 Hz frequency range experienced a decrease in power throughout the entire transition period.

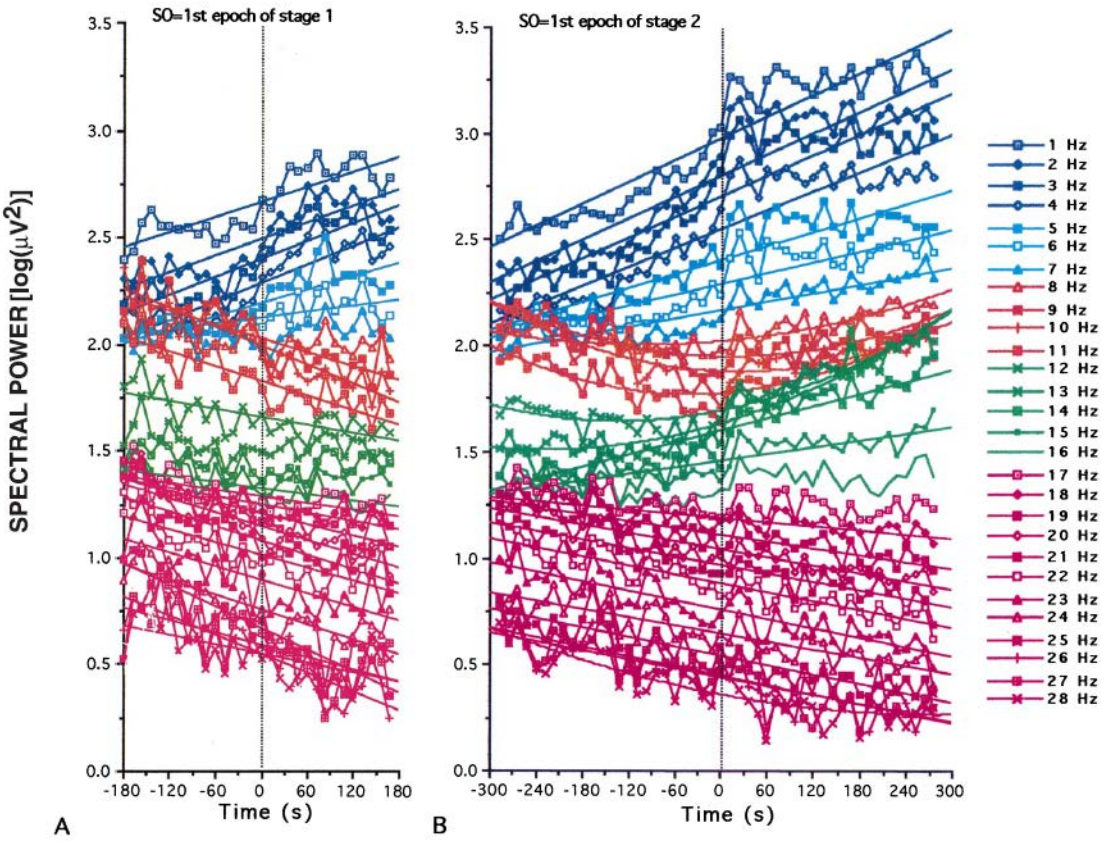

Figure 12. EEG power of 1 Hz bins from 1-30 Hz across the awake to sleep stage 1 transition and stage 1 to stage 2 transition. Reprinted with permission from [4].

To obtain a more in depth comparison of the change in power values across the frequency spectrum during the stage 1 transition, power values of each 1 Hz bin before thet first epoch of stage 1 were compared to the ones after it using one way repeated measure ANOVAs. A one way ANOVA (analysis of variance) is a technique for comparing the means of two or more samples of data.

It can be observed from Figure 13 that significant differences in EEG power existed across the 1-5 Hz range, with higher EEG power values after the stage 1

transition. In the 9-11 Hz and 20-28 Hz ranges, EEG power decreased after the transition. No significant differences were found for the 6-8 Hz, 12-19 Hz, and 29-30 Hz ranges.

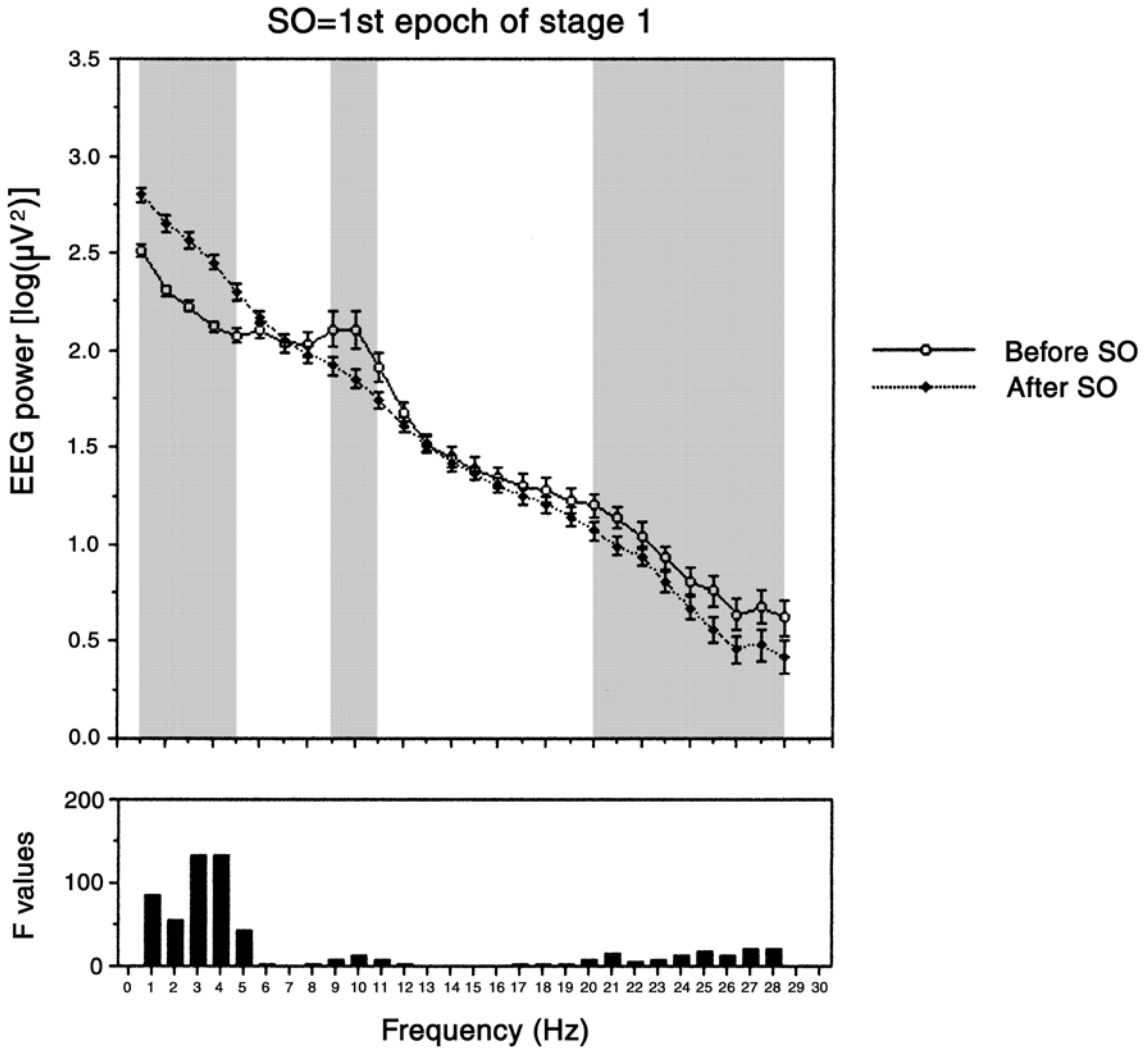

Figure 13. Mean power values for each 1 Hz frequency before and after the awake to sleep stage 1 transition. Reprinted with permission from [4].

The bottom plot of Figure 13 shows the corresponding F values of the ANOVA test. The F value, or F-statistic represents the statistical significance between two values, in this case it is a measure of how significant the 1 Hz EEG power differences are before and after sleep onset. A larger F value represents a greater significant difference between 1 Hz EEG power values before and after stage 1 onset [4]. The same analysis was also performed with stage 2 sleep defined as sleep onset, the results are displayed in Figure 14. Significant differences were discovered for the 1-8 Hz and 12-16 Hz ranges, both of which showed higher EEG power levels after the stage 2 onset. Meanwhile the 18-28 Hz range displayed lower power levels after the transition [4].

Furthermore, principal component analysis was performed on the 1 Hz power values in the 5 minutes before and after the stage 2 onset. A cumulative 90% of variance was explained by the first three factors extracted in the analysis corresponding to eigenvalues greater than 1. Table 3 details the factor loadings obtained from the analysis after varimax rotation and the percentage of variance explained by each factor. Factor 1 included the 1 Hz bins in the 17-28 Hz frequency range and explained 40% of the variance, Factor 2 included the 1-7 Hz as well as the 12-16 Hz frequencies and explained 35% of the variance, and the last factor included the 8-11 Hz frequencies while explaining 14% of the variance. With regards to traditionally defined EEG frequency bands, Factor 1 corresponds to the beta band (16-30 Hz), Factor 2 is composed of the delta (1-3 Hz), theta (4-7 Hz), and sigma bands (12-14 Hz), and lastly Factor 3 makes up a portion of the alpha band (8-12 Hz) [4].

Based on the results of the principal component analysis, 1 Hz power values were grouped together by averaging them together in the following ranges: 1-7 Hz, 8-11 Hz, 12-16 Hz, and 17-28 Hz. Figure 15 shows the time course of the power values for these bands during the awake-stage 1 transition and also the stage 1-stage 2 transition.

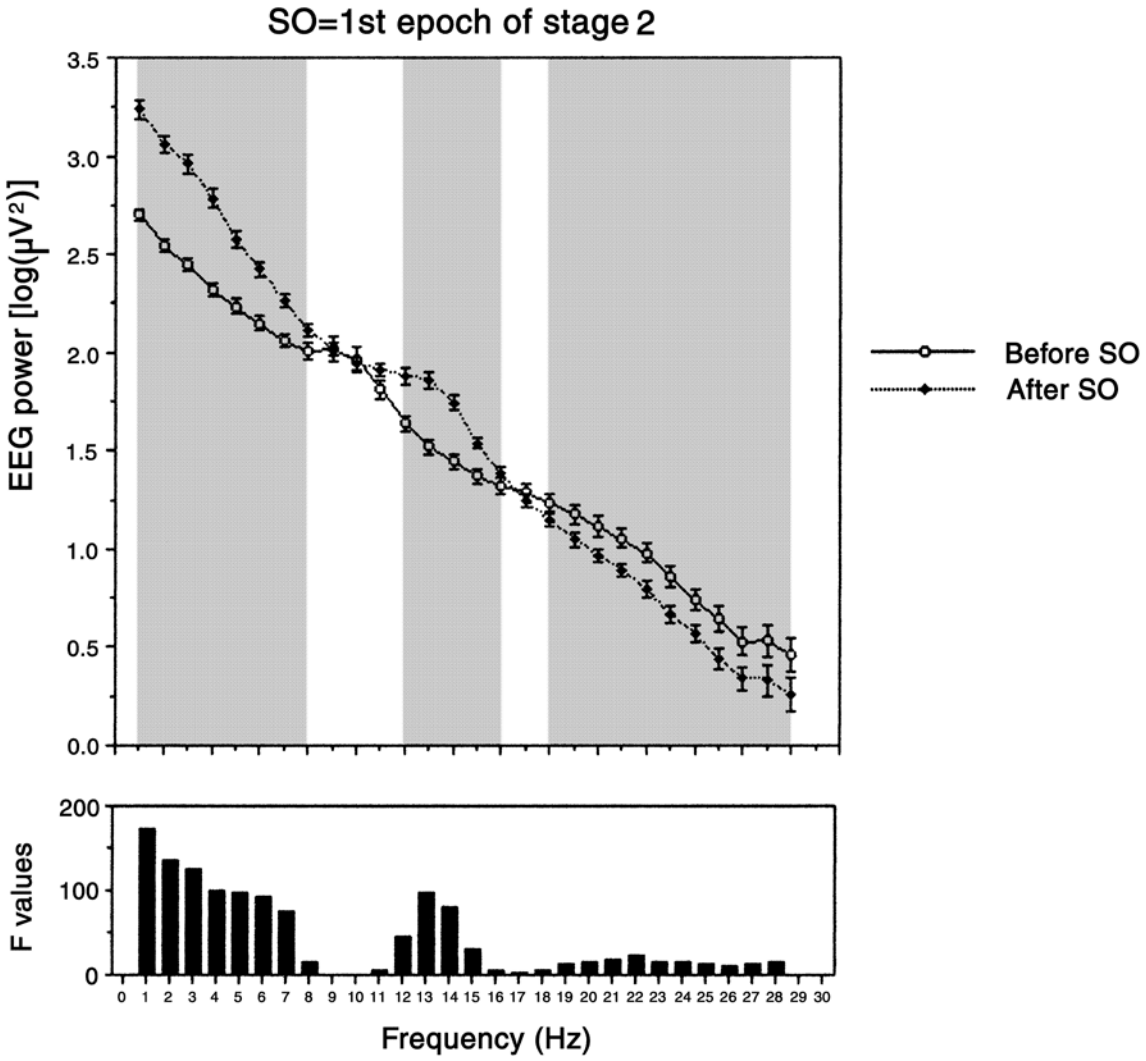

Figure 14. Mean power values for each 1 Hz frequency before and after the awake to sleep stage 1 transition. Reprinted with permission from [4].

The averaged power of the frequencies grouped within Factor 1 steadily decreased throughout the entire transition. Frequencies grouped into factor 2 progressively increased throughout the entire transition. Factor 3 and its corresponding frequencies decreased until the onset of stage 2 sleep, after which it begins to increase. Mean EEG power calculated across the various grouped frequency bands both before and after stage 1 and stage 2 sleep onset are shown in Figure 16.

Variable	Factor 1	Factor 2	Factor 3
1 Hz	−0.558955	*−0.808438*	0.023898
2 Hz	−0.548959	*−0.816616*	−0.055045
3 Hz	−0.565829	*−0.804861*	−0.077569
4 Hz	−0.570631	*−0.805270*	−0.069183
5 Hz	−0.508618	*−0.833704*	−0.036350
6 Hz	−0.449033	*−0.862582*	0.131050
7 Hz	−0.424454	*−0.814810*	0.326446
8 Hz	−0.240773	−0.597667	*0.665444*
9 Hz	0.341761	0.000693	*0.906632*
10 Hz	0.360983	0.123590	*0.879857*
11 Hz	−0.111613	−0.310709	*0.901980*
12 Hz	−0.395274	*−0.660302*	0.587736
13 Hz	−0.510722	*−0.710053*	0.442031
14 Hz	−0.462058	*−0.760329*	0.410611
15 Hz	−0.343780	*−0.841314*	0.295323
16 Hz	0.232814	*−0.706160*	0.408374
17 Hz	*0.845237*	−0.089204	0.348956
18 Hz	*0.891181*	0.153850	0.033159
19 Hz	*0.867608*	0.360639	0.036306
20 Hz	*0.811718*	0.468265	0.145141
21 Hz	*0.807531*	0.491430	−0.015927
22 Hz	*0.802756*	0.502496	−0.070506
23 Hz	*0.870824*	0.391979	−0.002059
24 Hz	*0.800292*	0.478031	−0.027493
25 Hz	*0.823059*	0.470328	0.012043
26 Hz	*0.853036*	0.310056	−0.022525
27 Hz	*0.707768*	0.529531	−0.024706
28 Hz	*0.718176*	0.527006	−0.039096
Explained variance (R^2)	0.402964	0.352089	0.141772

Table 3. Factor loadings of the principal component analysis carried out on the power values calculated across a 1–28-Hz frequency range at 1-Hz resolution during the sleep stage 1 to sleep stage 2 transition. Reprinted with permission from [4].

For when stage 1 is defined as sleep onset the EEG power in the delta and theta bands increased during the transition while EEG power decreased across the alpha, sigma, and beta bands. When stage 2 is defined as the onset of sleep EEG power increased across the delta, theta, alpha, and sigma bands while EEG power in the beta band decreased after the transition [4].

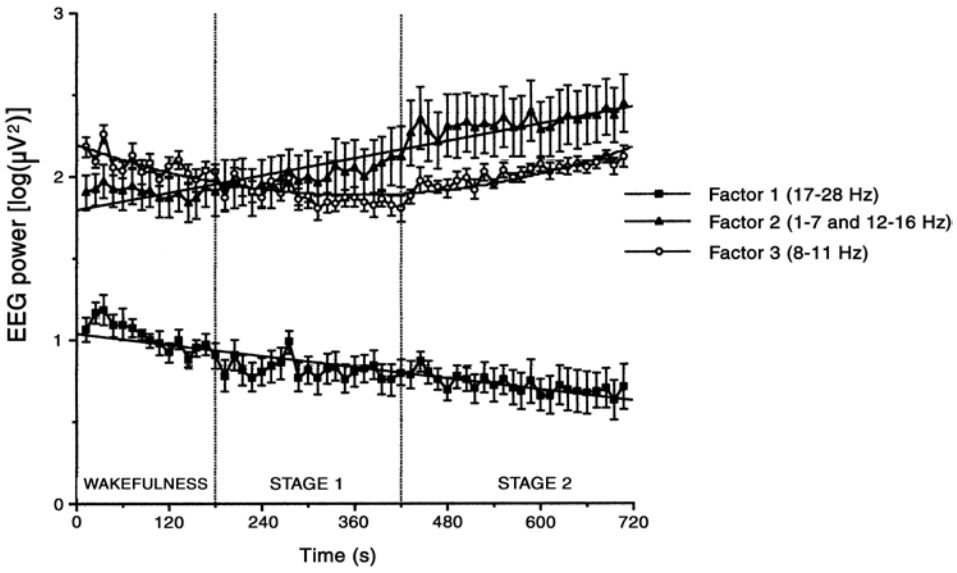

Figure 15. EEG power of the grouped frequency bands during the wakefulness-sleep transition. Reprinted with permission from [4].

This study also confirmed previous reports by Wright et al that the largest increase in EEG power occurred at the 3 Hz and 4 Hz frequencies while the greatest decrease occurred in the 9 Hz, 10 Hz, and 11 Hz frequencies during the awake-stage 1 transition [4]. Specifically, the 3 Hz and 4 Hz frequencies experienced an increase of

15.25% and 15.56% respectively, while the 9-11 Hz frequencies showed a 9%, 11.9%, and 8.9% decrease respectively during the transition.

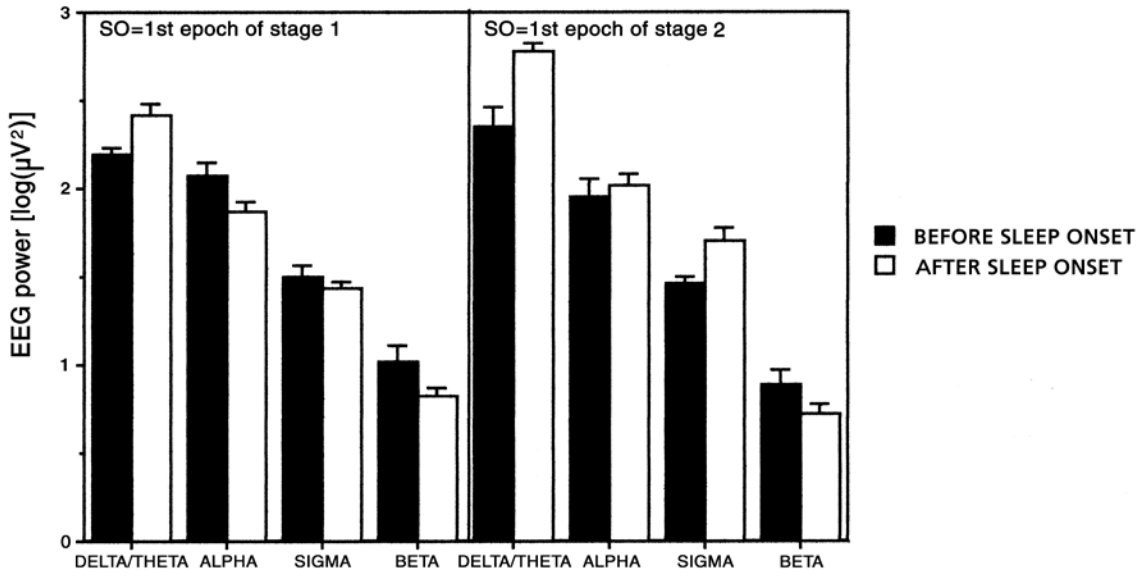

Figure 16. Mean EEG power calculated across the respective EEG bands before and after sleep onset. Reprinted with permission from [4].

The most important discovery achieved through this study was the changing behavior of the alpha frequencies during the stage 1 to stage 2 transition. While the delta, theta, sigma, and beta bands all exhibited a linear increase or decrease in EEG power across the entire transition from awake to stage 1 and stage 2, the power in the alpha band decreased across the stage 1 transition as expected. However its increase in power after the stage 2 transition suggests the existence of a different alpha activity associated with sleep maintaining processes. Further study of the phenomena in the alpha band is needed.

3.3 EEG phenomena within the alpha band during sleep onset

The alpha rhythm has become one of the fundamental features of human EEG as well as one of the most studied electrophysiological phenomena in humans since its discovery. It is characterized by its topographical distribution, frequency range, and reactivity. It achieves its maximum amplitude over occipital regions, covers the 8-13 Hz frequency range, and is highly correlated with eye opening and closing.

Traditionally, quantitative EEG studies of sleep in humans have mainly been focused on rough descriptions and characteristics of specific sleep stages. In contrast, considerably less effort has been devoted to the study of the electrophysiological properties of transient phenomena during sleep. For example, during the same sleep stage different EEG sleep events such as delta waves and K-complexes overlapping in frequency can both appear.

3.3.1 Spectral composition and topographical distribution

Using brain mapping techniques, Cantero et al discovered that the alpha frequencies showed a similar topographical distribution across the awake, drowsiness, and REM sleep stages [2] (Figure 17).

In all three sleep states the power in the alpha band peaked over occipital regions and displayed a progressive decrease of power anterior cortical. On the other hand the spectral composition of the alpha band was different across the three states (figure 17). Spectral energy within the middle alpha (9.5-11 Hz) decreased significantly from wakefulness to REM sleep, with the fast alpha band (11.5-13 Hz) capable of clearly distinguishing between awake and sleep states. However, the slow alpha band (7.5-9 Hz)

showed similar energy across awake and sleep stages except between wakefulness and drowsiness in the parietal and occipital regions. This suggests the slow alpha band is governed by common neural synchronization mechanisms.

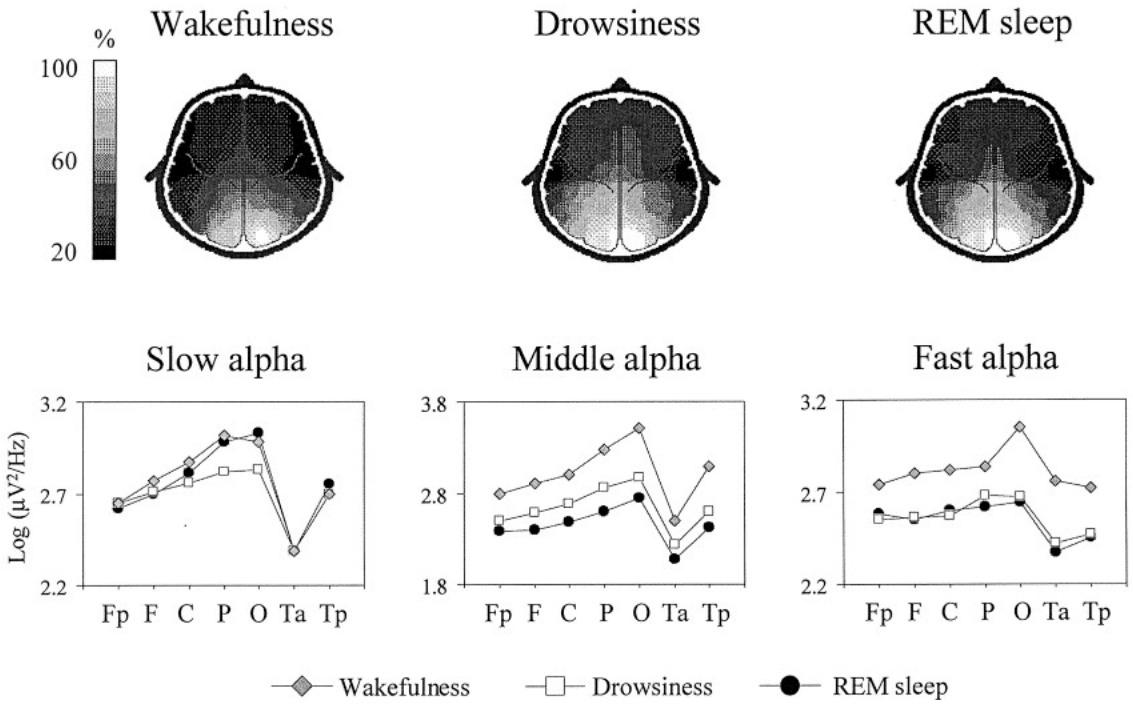

Figure 17. Top: Topographic representation of scalp-recorded alpha activity during relaxed wakefulness, drowsiness period, and REM sleep. Bottom: Spectral contribution of each human alpha variant considering three alpha subdivisions (slow: 7.5–9 Hz; middle: 9.5–11 Hz; fast: 11.5–13 Hz) and different scalp areas (prefrontal, frontal, parietal, occipital, anterior and posterior temporal). Reprinted with permission from [2].

Determining the spectral differences between cortical activities that overlap the same frequency range requires examining the EEG spectral microstructure at a higher

resolution than what is achievable through traditional broadband definitions. High resolution spectral procedures have been shown to provide greater sensitivity than broadband models in various applications such as abnormal oscillation detection in epilepsy, characterization of brain changes during the wakefulness to sleep transition, and in discriminating between different types of sleep spindles [2].

Correlation strength between hemispheric local alpha coherence in wakefulness, drowsiness, and REM sleep were explored topographically (Figure 18). Functional association levels between the cortical regions were obtained using a bivariate partial correlation analysis. The thickness of the black lines in figure 18 correspond with their respective correlation values. The high bi-directional anterior-posterior correlation during wakefulness suggests active feedback between these areas in this state.

A decrease of the frontal-occipital correlation in alpha during drowsiness was only observed in the posterior to anterior direction, suggesting that activation of the frontal cortical circuits involved in the generation of this pattern is mostly independent of the occipital populations [2]. The activation of frontal-central cortical circuits could be the result of a variety of brain mechanisms for entering or maintaining sleep, in which case the anterior alpha activity would be independent of the alpha rhythm in the awake state and functionally correlate with the drowsiness process. This scenario is consistent with literature in that anterior alpha is associated with sleep maintaining processes while occipital alpha is functionally related to the awake state. Thus the appearance of occipital alpha activity during sleep is often interpreted as an arousal response [2].

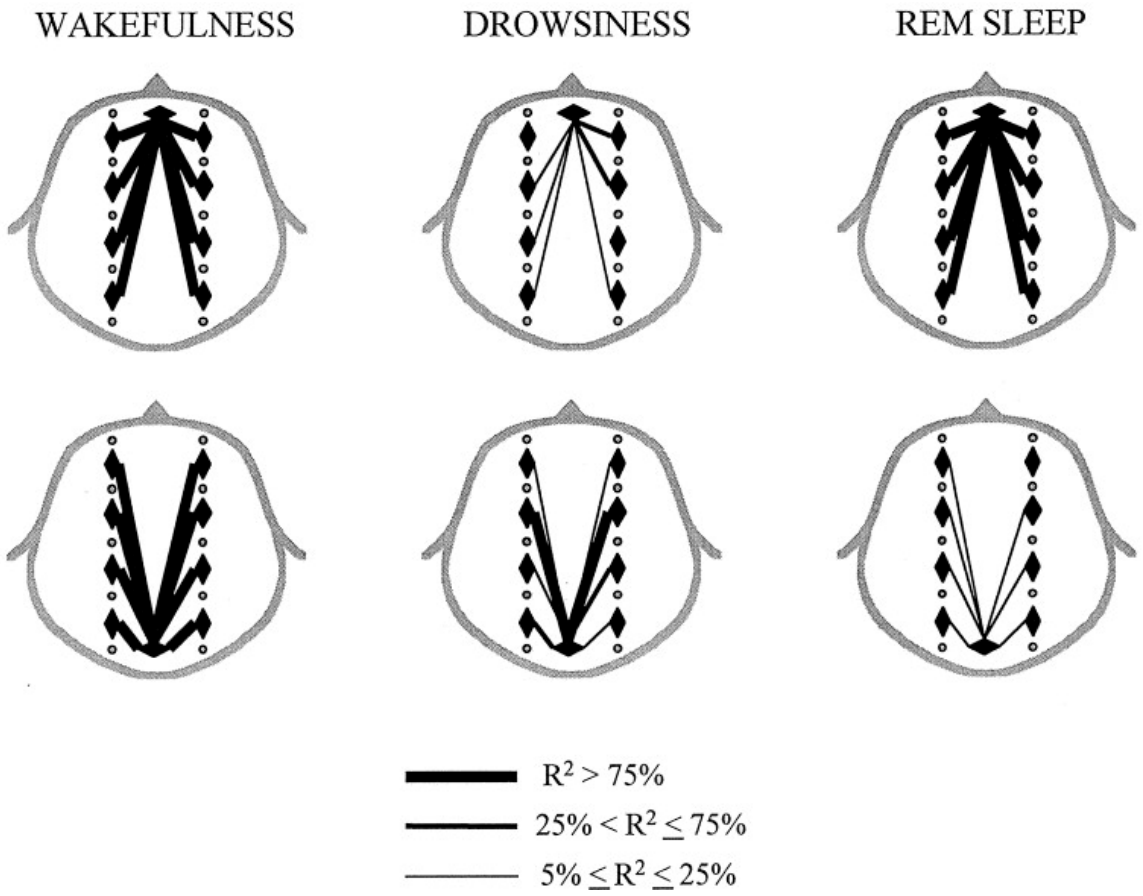

Figure 18. Topographic representation of the correlation strength between inter- and intra-hemispheric local alpha coherence during alpha rhythm in relaxed wakefulness, alpha activity at sleep onset, and REM-alpha bursts. Reprinted with permission from [2].

4. SUPPORT VECTOR MACHINES

Support vector machines (SVM) are supervised learning models with algorithms which analyze data and recognize patterns that is useful for classification problems [17]. Provided with a set of training samples, each belong to one of two categories, an SVM training algorithm builds a model representing the training samples as points in space. The points are mapped in such a way that the samples from the two categories are divided by an optimal hyperplane, forming the largest possible gap between samples from the separate categories. A new set of samples can then be mapped to the same space and predicted to belong to a category based on which side of the hyperplane they lie.

4.1 Linear SVM

Given a set of training data D, a set of n points of the form

$$D = \{(x_i, c_i) | \, x_i \in R^P, c_i \in \{-1,1\}\}_{i=1}^{n} \tag{7}$$

where each x_i is a P-dimensional real number or vector and c_i is the label indicating the class to which the point x_i belongs. The goal is to find the maximum margin hyperplane that divides the points with $c_i = -1$ from those with $c_i = 1$ [15]. A hyperplane can be written as the set of point x satisfying

$$w \cdot x - b = 0$$

where $\cdot$ denotes the dot product. w is a surface normal vector perpendicular to the hyperplane. The offset of the hyperplane from the origin along w is given by

$$\frac{b}{\|w\|}$$

To maximize the margin between the parallel hyperplanes separating the two classes of data, w and b are chosen such that

$$w \cdot x_i - b = -1$$

and

$$w \cdot x_i - b = 1$$

For linearly separable data, the two hyperplanes can be chosen so that there are no points between them and then try to maximize the distance their distance. The distance between the two hyperplanes is given by

$$\frac{2}{\|w\|}$$

So the term to minimize is $\|w\|$. To prevent data points from falling into the margin, a constraint is added such that

$$w \cdot x_i - b \leq -1$$

or

$$w \cdot x_i - b \geq 1$$

for x_i of the two classes. These can be rewritten as

$$c_i(w \cdot x_i - b) \geq 1, \ 1 \leq i \leq n \tag{8}$$

The SVM training optimization problem is therefore given by

$$\min_{w,b}\|w\| \tag{9}$$

subject to

$$c_i(w \cdot x_i - b) \geq 1 \tag{10}$$

This is also referred to as the primal form and is a quadratic optimization problem [15]. See figure 19 for a graphical example of SVM training.

4.2 Soft margin SVM

For cases where there exists no hyperplane that can separate the data points from the two categories, a soft margin approach can be adopted in order to establish a hyperplane that splits the points from the separate classes as cleanly as possible while still maximizing the distance to the nearest cleanly split data points [15]. The slack variables ξ_i are introduced which measure the degree of misclassification of each x_i. Equation 8 then becomes

$$c_i(w \cdot x_i - b) \geq 1 - \xi_i, \ 1 \leq i \leq n \tag{11}$$

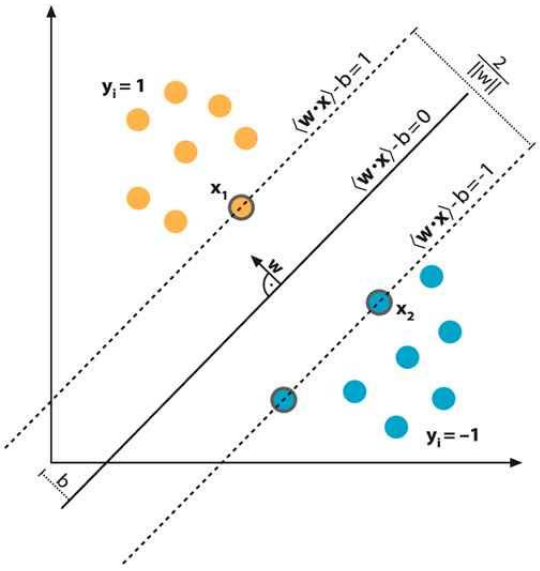

Figure 19. SVM training to find the optimal hyperplane (solid black line) which separates the samples from two classes (orange and blue circles) with maximum margin. Support vectors are represented by circles with outlines. Reprinted with permission from [19]. © 2013 IEEE.

The objective function thus changes as the optimization now involves a tradeoff between a large margin and a small error. For a linear penalty function the optimization problem becomes

$$\min_{w,\xi} \frac{1}{2}\|w\|^2 + C\sum_{i=1}^{n}\xi_i \qquad (12)$$

subject to

$$c_i(w \cdot x_i - b) \geq 1 - \xi_i, \;\; \xi_i \geq 0$$

where C is the constant cost coefficient.

The solution w can also be represented as a linear combination of the training points:

$$w = \sum_{i=1}^{n} \alpha_i c_i x_i$$

Substituting for w in (9) and (10) gives an equivalent optimization problem over α_i instead of w. This is known as the dual form and is given by

$$\max_{\alpha_i} \sum_{i=1}^{n} \alpha_i - \frac{1}{2}\sum_{i,j} \alpha_i \alpha_j c_i c_j \, (x_i \cdot x_j) \qquad (13)$$

subject to

$$0 \leq \alpha_i \leq C$$

and

$$\sum_{i=1}^{n} \alpha_i c_i = 0$$

4.3 Non-linear SVM

In the case of non-linearly separable data, a non-linear classifier can be created by applying kernel functions [15]. The original data points are mapped to a higher order feature space and (13) can be written as

$$\max_{\alpha_i} \sum_{i=1}^{n} \alpha_i - \frac{1}{2} \sum_{i,j} \alpha_i \alpha_j c_i c_j \, k(x_i, x_j) \qquad (14)$$

where $k(x_i, x_j)$ is the kernel function representing the inner dot product of the training points x_i and x_j. Different kernel functions can be applied by mapping $k(x_i, x_j)$ to different functions. One widely used kernel is the Gaussian or RBF (radial basis function) kernel, with the following mapping:

$$k(x_i, x_j) = \exp\left(-\gamma \left\| x_i - x_j \right\|^2\right), \ \gamma > 0 \qquad (15)$$

4.4 Parameter selection

The effectiveness of an SVM classifier depends on the selection of the kernel, the kernel's parameters, and the soft margin cost C. For the Gaussian kernel, the two parameters γ and C are often selected by a grid search with exponentially growing sequences of γ and C. The combination of the parameters which gives the best accuracy are selected for training.

4.5 Performance evaluation of SVM classifiers

Accuracy, precision, and recall are all statistical measures of the performance of a binary classification test. All possible outcomes of such a test can be re represented by a confusion matrix as shown in figure 20 Precision, recall (sensitivity), and accuracy are given by the following equations:

$$\text{Precision} = \frac{true\ positive}{true\ positive + false\ positive}$$

$$\text{Recall (sensitivity)} = \frac{true\ positive}{true\ positive + false\ negative}$$

$$\text{Accuracy} = \frac{true\ positive + true\ negative}{true\ positive + false\ positive + true\ negative + false\ negative}$$

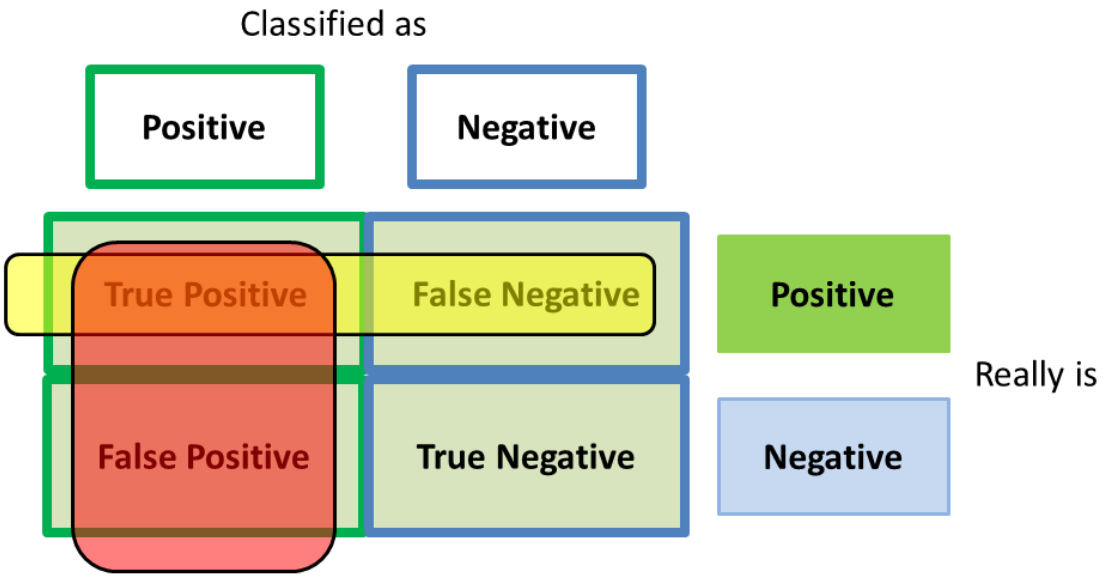

Figure 20. Confusion matrix; precision in red, recall in yellow. Reprinted with permission from [19]. © 2013 IEEE.

Precision is defined as the proportion of true positives against all the positive results (both true positives and false positives), in other words it represents the relevance of the positive classification. Recall, or sensitivity, on the other hand is defined as the proportion of positive samples that are correctly classified. In other words, it is a measure of the test's ability to detect positives. Finally, accuracy is the proportion of true results, both true positives and true negatives, in the set.

5. APPROACH[*]

The following sections cover the proposed approach to drowsiness detection.

5.1 EEG database

PhysioBank is an online database that offers free access to a large and growing archive of well-characterized set of digital recordings of physiologic signals and related data for use by the biomedical research community [6]. For the purpose of our study we needed reliable data collected using high quality recording devices with epochs classified into their respective sleep stages by experts. These stringent requirements are to reduce potential errors introduced in the raw signal using unverified off-the-shelf EEG devices, as well as manual classification errors made by non-experts. PhysioBank is perfect in this regard as most of the available data sets were collected for the purpose of studies in research institutes and therefore should be of high quality. The particular database we use is the CAP Sleep Database [4], which at the moment contains 108 EEG recordings registered at the Sleep Disorders Center of the Ospedale Maggiore of Parma, Italy. Subjects were recorded during a normal night of sleep, with the recordings provided in the widely used EDF format. The waveforms contain at least three EEG channels as well as EEG bipolar traces according to the international 10-20 system. 16 recordings were collected on healthy patients who did not have any neurological

[*] Reprinted with permission from Shaoda Yu, Peng Li, Honghuang Lin, Rohani, E., Gwan Choi, Botang Shao, Qian Wang, "Support Vector Machine Based Detection of Drowsiness Using Minimum EEG Features", Social Computing (SocialCom), 2013 International Conference on Social Computing, 827-835, 8-14 Sept. 2013.Copyright 2013 IEEE

disorders and were free of drugs affecting the central nervous system. 92 recordings were collected from patients with various disorders such as insomnia and narcolepsy.

Expert neurologists trained at the Sleep Center manually scored the EEG recordings into their respective sleep stages according to the Rechtschaffen and Kales standard for each 30 second epoch.

5.2 SVM classification flow

We use the 16 recordings of healthy subjects from the CAP Sleep Database mentioned previously to train and test our SVM classifiers. First, we identify the feature set with the best classification accuracy between awake and drowsy (sleep stage 1) states. Afterwards, we extend the drowsy state to include sleep stage 2. By effectively combining both of these sleep stages to represent the drowsy state we remedy the problem of an unclear definition of drowsiness with respect to the defined sleep stages. Our SVM based classification flow consists of data preparation, feature extraction and selection, SVM training and testing, and evaluation of results, which is shown in figure 21. The key steps of the flow are described in detail below.

5.3 EEG based SVM classifiers

For best performance and thorough test of our classifier, we evenly divide the data points amongst the two sets. Random partition of the data for training and testing is performed in order to run multiple tests of the same data using different data set configurations to get the average performance of the SVM classifiers.

Due to the small amount of data available for a single subject it is necessary to combine training and testing data from multiple subjects in order to get a respectable

number of training and testing samples for SVM to give a reliable result. Therefore normalization techniques need to be implemented to account for the inherent differences in brain signal levels as well as other environmental factors across different patients and recordings. A simple method that has proven to be effective was chosen. First we assume that at the beginning of recording all patients are awake for at least 5 minutes.

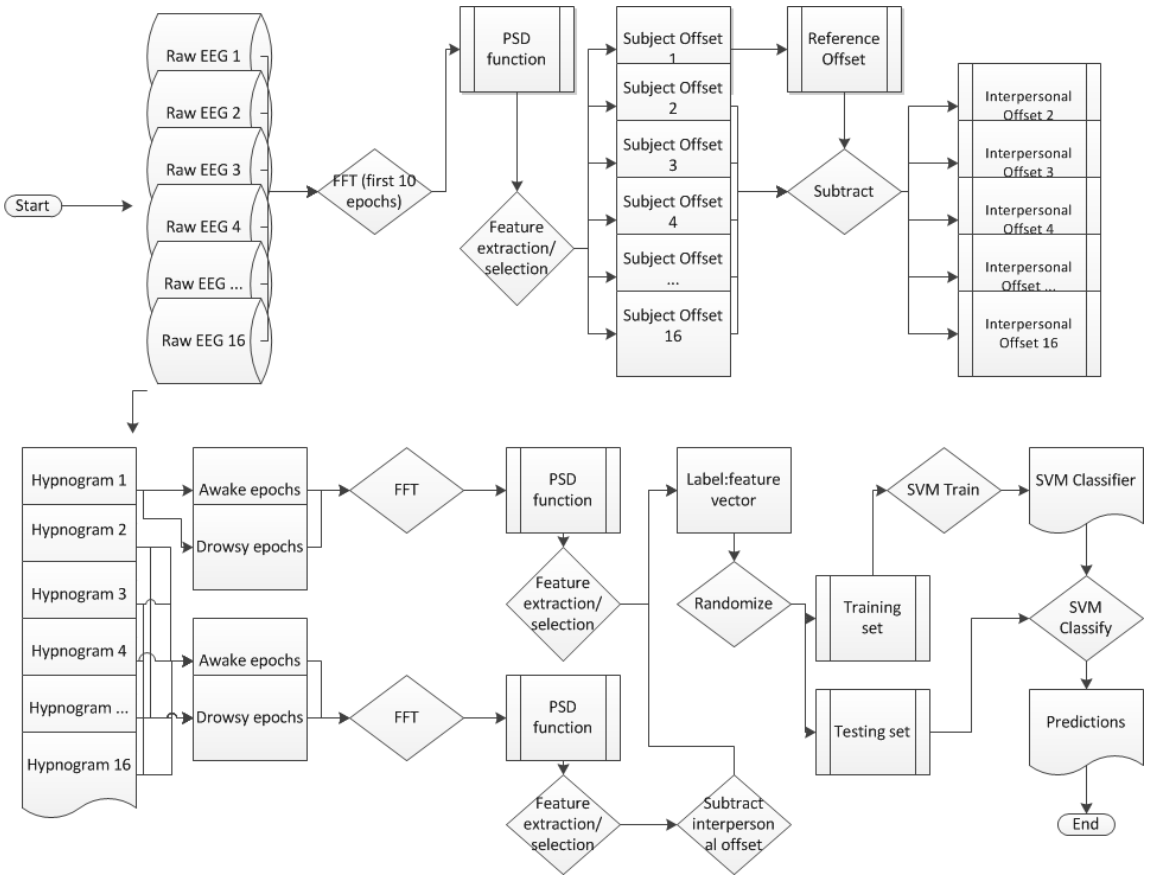

Figure 21. SVM based classification flow. Reprinted with permission from [19]. © 2013 IEEE.

Then we select one patient to use as a reference by taking the FFT of the EEG over the first 5 minutes and calculating the average power or value for the features we plan to extract from the signal. The same calculation is performed for the other patients. The difference in the power or value of every feature between each patient and the reference for the 5 minute interval is used as an offset between the respective patient and the reference, and all further feature extraction account for that offset. As will be demonstrated later in the results section, this method is very effective.

The SVM program we use is the SVM-Light package by Joachims [7]. SVM-Light is an implementation of SVM in C and offers a fast optimization algorithm that can handle large data sets, and has support for many standard kernel functions. We used the default parameters in training SVM-Light except for the kernel function and the C parameter. We used the RBF (Radial basis function) kernel over the default linear kernel as our problem is non-linear by nature. C is a regularization parameter; a small C allows training errors to be more easily ignored, resulting in a larger margin, whereas a large C makes training errors harder to be ignored, giving a narrow margin. We choose the value of C that yields the least error and highest precision during training. This is done by initially training using a small C, which is increased until further improvements in training accuracy is not possible. We have found 4000 to be the optimal value for C.

5.4 Feature extraction and selection

Feature extraction transforms the raw sensor readings from the EEG recording devices into a feature vector from which we can then perform feature selection. As discussed earlier, feature selection is the key focus of this work. Previous studies utilize

the full bands in their models but new evidence from the neuroscience community suggests that sub-banding can be useful in selecting the critical sub-bands which provide the greatest differentiability between the awake and drowsy states. As far as SVM is concerned, it tries to establish a hyperplane that separates the two classes with the greatest distance between them. So, intuitively critical sub-banding should help in this regard by removing redundant data that does not help to establish this optimal hyperplane.

5.4.1 Classifiers based on a large space of 1hz sub-band features

To systematically examine the potential benefits of sub-banding, we train a large number of SVM classifiers with varying numbers of 1Hz subband features. We also try to find the optimum feature set among this set of classifiers by initially training and testing our SVM model using the full set of 30 features comprised of the average power from 1-30 Hz in 1 Hz resolution bin. We then remove a feature after each run and observe the resulting impact on classification accuracy. The optimum feature set is essentially the least number of features that can still yield a high classification accuracy. The optimal set of sub-band features found through this brute-force search also provides a reference for evaluating our neuroscientifically motivated feature set described below.

5.4.2 Neuroscientifically motivated feature set

Based on neuroscience studies of Gevins, Gennaro, and Klimesch et al [4] [5] [8] we extract 9 features based on the PSD of the EEG for each epoch: The average power of 1-4 Hz in 1 Hz resolution bin, the average power of 9-11 Hz in 1 Hz bin, the ratio of the average power in delta to the average power in alpha, and the ratio of the average

power in theta to the average power in alpha. Here we define delta to be 1-5 Hz, theta to be 5-8 Hz, and alpha to be 8-12 Hz in the traditional broadband manner.

Seven of these features are essentially sub-banded versions of the traditional delta and alpha bands; the neuroscience research by Gennaro et al show that certain frequencies within a band experience a greater increase or decrease in power compared to its adjacent frequencies [4]. Specifically the greater decrease in power of the 9, 10, and 11 Hz frequencies in alpha, as well as greater increase in power of the 3 and 4 Hz frequencies in delta/theta. The remaining two features utilize the fact that during the transition from awake to stage 1 sleep, the power of delta and theta increases while the power of alpha decreases, both in a linear fashion. Therefore the ratio between them will decrease as the subject approaches stage 1 sleep (See Fig. 15).

We now try to provide further insight into the optimum feature set and how these features correlate with biomedical evidence. The two traditional features (power of delta/alpha, power of theta/alpha) in the optimum feature set captures the general behavior of these bands during the awake-sleep transition. During the transition from awake to sleep stage 1 the power of alpha decreases while the power of theta and delta increases, therefore the ratios will reflect this. The next four features, 1-4 Hz in 1 Hz resolution, span the entire delta (1-3 Hz) range as well as the lower portion of theta (4-7 Hz). The choice to include only a small part of theta is due partly to experimental results that find the largest increase in EEG power during the awake-sleep transition to occur at 3 and 4 Hz [4] [16]. The other reason is due to the unclear boundary between theta and alpha as a result of interpersonal variability; upper theta and lower alpha can potentially

overlap and mask each other. By deliberately excluding upper theta we attempt to avoid this problem. The final three features, 9-11 Hz in 1 Hz resolution, cover part of lower alpha (7.5-11.5 Hz). For the same reasons as before these features were selected partly based on studies that find the greatest decrease in EEG power during the awake-sleep transition to occur at 9, 10, and 11 Hz [4] [8] [16], and once again the lower part of alpha is excluded to allow for a buffer zone from upper theta.

6. EXPERIMENTAL RESULTS*

6.1 Sub-banding based SVM classifiers with 1hz resolution

Our foregoing discussions suggest sub-banding can be highly effective for feature selection and may circumvent many limitation of the traditionally broadband features. To closely examine the performance of subbanding, we train a large number of classifiers with varying numbers of 1Hz subband features. The results of these SVM classifiers are shown in Tables 4 and 5. When the full feature set of 30 features are used SVM is able to achieve very high accuracy (over 95%) and precision (over 90%). As the number of features are reduced these accuracy levels hold steady all the way to when just 9 features are used, and accuracy degradation occurs from that point on. It is also interesting to note the correlation between the number of support vectors established and the performance of the SVM; a low number of support vectors yield very high classification accuracy while the opposite is true for a high number of support vectors. The reason is because as the feature vector is reduced the mapping dimension is also reduced, which essentially means that even though SVM has to work harder and longer (more support vectors), it will not be able to achieve very high accuracy because the dimension space is simply not large enough to find the optimal hyperplane. The performance of the classifier does not decrease monotonically as the feature set shrinks, this is partly because of the un-proportional number of awake and drowsy samples in the

* Reprinted with permission from Shaoda Yu, Peng Li, Honghuang Lin, Rohani, E., Gwan Choi, Botang Shao, Qian Wang, "Support Vector Machine Based Detection of Drowsiness Using Minimum EEG Features", Social Computing (SocialCom), 2013 International Conference on Social Computing, 827-835, 8-14 Sept. 2013. Copyright 2013 IEEE

testing set as well as the ability of the classifier to classify negative samples more accurately. The awake samples outnumber the drowsy samples by a factor of 2.6 in this experiment, and coupled with the fact that our classifier is very good at classifying negative samples under almost any circumstance the overall accuracy and precision levels do not vary much as the number of features decreased. The more important metric to consider in this case is recall, the ability to correctly classify positive samples. As expected recall had a much greater variance across the test cases.

These results also suggest that after a certain point increasing the feature set further will no longer positively affect classification performance; but could lead to overfitting. These are redundant features that increase the feature set without making any contribution. Therefore it will be greatly beneficial to identify a subset of features that provide near optimum classification performance as well as keeping the feature set size to a minimum.

6.2 Performance of the proposed features

Table 6 show the results when average power in the traditional bands are used as features compared with our proposed features which incorporate subbanding. Clearly techniques involving traditional frequency bands are poor when used with SVM. This may be due to any number of factors, one being the low dimension space as previously observed, and another being the low resolution spectral analysis when multiple frequencies are combined and considered as one band. Our proposed set of 9 features on the other hand performed extremely well, on par or better than the best results seen in the test to find the optimum feature set in Tables 4 and 5. Therefore we select it as the

optimum feature set as determined by manual feature selection. One interesting observation that can be made is that the ratio of the average power in delta to the average power in alpha is a more useful feature than the ratio of the average power in theta to the average power in alpha for drowsiness detection. This suggests that there exists greater differentiability power in delta between the awake and drowsy states. Our results for this test show that the highest classification accuracy and precision achieved was 97.64% and 96.91% respectively, using the average power from 1-8 Hz in 1 Hz bin resolution as features. Our proposed feature set achieved an accuracy and precision of 97.48% for both fields while incurring lower training error. This suggests that our proposed feature selection scheme is optimal for EEG drowsiness detection using SVM.

Finally we test our SVM model for the case when both sleep stages 1 and 2 were combined to form the drowsy state. The results are summarized in Table 7. The results indicate that our SVM model is able to distinguish between awake and sleep stage 1 as well as between awake and sleep stage 2 with high accuracy. In comparison with the previous case where only sleep stage 1 composed the drowsy state (Tables 4-6), two differences are worthwhile to note: the slightly higher training precision and the significantly higher number of support vectors established by SVM. The former may be explained by the larger training set used (3095 vs. 217 drowsy states) while the latter is most likely a result of the two sleep states (stage 1 and stage 2) occupying different regions in the dimension space, which when combined into a single label (drowsy) produces more support vectors. It can also be observed that in this case the traditional broadband features actually performed on par with the subband features. To explore this

further we cut the number of drowsy samples in the training and testing sets down to 217, the same amount used previously to classify between awake and stage 1, in order to get an even comparison. We select a single feature set for each feature selection method (broadband or subband) for this test since the feature sets within a method did not differ much in previous results. Table 8 illustrates that even though both feature selection methods produce poor recall, the subband features are still superior in terms of overall accuracy, precision, and recall.

We believe that the poor recall is due to an insufficient amount of training data, so to test this we incrementally increase the amount of drowsy samples in the combined model from 217 to the full 3095 and observe the effect of classification performance. Fig. 5 shows the resulting recall vs. sample size graph. A logarithmic increase in recall is observed as sample size increases. We are able to achieve 90% recall using only 1500 training and testing samples, or about half of the total samples.

Features	Training error(%)	Training precision(%)	Test accuracy(%)	Test precision(%)	Test Recall(%)	# support vectors
1-30 Hz	8.76	82.33	96.09	93.56	94.64	60
1-29 Hz	7.13	83.41	95.97	91.03	98.2	58
1-28 Hz	7.56	82.75	96.59	90.88	97.33	58
1-27 Hz	8.98	81.98	97.48	92.09	97.6	54
1-26 Hz	8.03	84.88	97.22	91.84	95.66	59
1-25 Hz	7.39	84.88	96.71	95.43	94.54	50
1-24 Hz	8.88	84.52	96.17	94.96	91.42	53
1-23 Hz	7.78	85.71	96.39	94.9	91.62	49
1-22 Hz	8.04	83.93	96.58	94.54	92.81	54
1-21 Hz	8.11	83.88	96.69	94.67	92.77	51
1-20 Hz	8.4	83.24	96.22	93.93	92.65	55
1-19 Hz	8.29	83.88	96.35	93.56	93.7	51
1-18 Hz	7.67	86.13	96.41	94.66	94.45	50
1-17 Hz	7.54	84.63	96.3	94.88	96.97	57
1-16 Hz	8.66	83.33	95.82	94.05	95.81	55
1-15 Hz	7.14	85.55	96.19	94.66	93.84	52
1-14 Hz	7.59	86.13	94.47	96.91	93.51	56
1-13 Hz	8.2	84.92	95.56	95.23	93.25	58
1-12 Hz	8.95	83.56	94.45	92.18	95.24	55
1-11 Hz	8.33	86.21	95.59	96.53	94.31	54
1-10 Hz	7.08	84.56	96.65	91.79	93.78	49
1-9 Hz	8.88	82.86	96.24	93.56	89.34	63
1-8 Hz	12.55	78.43	94.34	93.56	87.56	73
1-7 Hz	13.42	74.56	89.73	88.42	86.67	88
1-6 Hz	17.21	67.64	88.82	88.19	86.34	110
1-5 Hz	20.45	61.78	86.45	86.53	78.54	126
1-4 Hz	24.54	53.54	87.12	86.23	77.43	165
1-3 Hz	34.56	34.34	80.42	85.33	78.94	210
1-2 Hz	45.96	17.67	80.86	84.97	25.73	279
1 Hz	54.45	6.32	75.73	67.85	20.43	438

Table 4. SVM results using sub-banding with 1 Hz resolution. (569 awake and 217 drowsy samples)

Features	Training error(%)	Training precision(%)	Test accuracy(%)	Test precision(%)	Test Recall(%)	# support vectors
26-30 Hz	43.17	24.77	77.39	78-14	44.78	258
21-30 Hz	15.66	71.02	92.55	90.96	82.64	93
20-30 Hz	16.74	68.8	94.28	92.61	88.17	98
19-30 Hz	15.13	72.69	95.28	94.77	90.98	94
18-30 Hz	12.44	78.93	95.24	94.73	91.02	75
17-30 Hz	11.71	78.88	94.96	93.48	90.42	73
16-30 Hz	11.91	76.58	91.09	92.81	89.76	78
15-30 Hz	11.21	78.85	95.81	94.73	92.83	65
14-30 Hz	11.34	77.57	95.97	93.68	92.39	71
13-30 Hz	10.86	78.7	96.46	93.83	94.96	69
12-30 Hz	10.91	78.66	96.46	94.09	95.1	68
11-30 Hz	10.87	79.88	96.8	93.94	94.72	70
10-30 Hz	10.42	80.13	97.11	93.33	94.51	68
21-25 Hz	34.1	36.23	89.55	90.19	74.85	211

Table 5. SVM results using sub-banding with 1 Hz resolution. (569 awake and 217 drowsy samples)

Features	Training error(%)	Training precision(%)	Test accuracy(%)	Test precision(%)	Test Recall(%)
α, β, δ, θ	45.56	19.19	78.89	60.88	70.55
α, δ, θ	43.73	21.28	80.1	67.32	48.24
α, β, δ	48.54	13.89	76.34	79.54	18.35
1-4 Hz, 9-11 Hz, δ/α, θ/α	9.67	83.24	97.94	98.73	93.41
1-4 Hz, 9-11 Hz, δ/α	9.17	83.68	95.86	97.35	91.54
1-4 Hz, 9-11 Hz, θ/α	12.64	74.66	94.58	95.78	89.45
1-4 Hz, 9-11 Hz	11.57	77.36	95.34	96.9	88.43

Table 6. SVM results using traditional EEG bands and proposed features [9] [11] [17]. (569 awake and 217 drowsy samples)

Features	Training error(%)	Training precision(%)	Test accuracy(%)	Test precision(%)	Test Recall(%)
α, β, δ, θ	8.18	95.51	98.34	98.22	99.67
α, δ, θ	9.78	94.44	97.97	97.47	99.55
α, β, δ	11.88	92.53	97.65	98.85	99.77
1-4 Hz, 9-11 Hz, δ/α, θ/α	7.26	95.86	98.2	97.88	99.83
1-4 Hz, 9-11 Hz, δ/α	7.75	95.6	97.97	98.01	99.2
1-4 Hz, 9-11 Hz, θ/α	7.84	95.22	98.01	97.87	99.47
1-4 Hz, 9-11 Hz	7.39	95.45	97.98	97.91	99.73

Table 7. SVM results using combined drowsy state. (569 awake and 3095 drowsy samples)

Features	Training error(%)	Training precision(%)	Test accuracy(%)	Test precision(%)	Test Recall(%)
α, β, δ, θ	19.64	66.25	75.31	56.76	48.8
1-4 Hz, 9-11 Hz, δ/α, θ/α	7.36	86.88	87.22	92.76	51.96

Table 8. Table 8. SVM results using combined drowsy state with reduced samples. (569 awake and 217 drowsy samples)

6.3 Comparison with prior work

In comparison with prior work our SVM based approach is superior to the threshold based methods in terms of classification accuracy (˜95% vs. ˜85%). Compared with the SVM based approach adopted by Yeo et al [17] our system achieves similar accuracy, but comes out on top with significant advantages in terms of flexibility as well as data storage and processing requirements. First of all, we do not employ any sort of pre-processing on the EEG waveform to remove artifacts while Yeo et al performed manual artifact removal. By removing artifacts they artificially create training and testing sets containing only data which are either clearly awake or drowsy with no ambiguous in-between states. Not only is this unrealistic, but also unfeasible in a real-time system without using automatic artifact removal algorithms. Our model which does not utilize artifact removal achieves very high accuracy, demonstrating the flexibility and robustness of our manual feature selection choice. Yeo et al's proposed feature set is composed of 304 features per sample (4 features x 4 frequency bands x 19 EEG channels) [17]. Our results indicate that we are able to achieve a close level of accuracy utilizing only 8 or 9 features per sample. This reduction in feature size can have significant implications on data storage and processing requirements, especially in a real time system.

7. CONCLUSION

In this thesis we first provide some background on EEG as related to drowsiness by reviewing biomedical evidence established by various studies. Then we gave an overview of existing work done in the area and the level of accuracy they achieved. Next we utilized quantitative EEG changes during the sleep onset transition to provide motivation for subbanding the traditional EEG frequency bands into smaller, higher resolution 1 Hz bin intervals to use as features for our SVM classifier. we also provide deeper insight into the feature selection choice and back them with biomedical evidence. we used scientific, public domain EEG databases to develop and test the system model. Techniques to account for interpersonal variability across the 16 subject recordings were developed and implemented.

To start we assume that the drowsy state is comprised of sleep stage 1 only and test our proposed feature set which incorporate subbands against traditional broadband EEG frequency bands using SVM and find that subbanding is critical to achieve high classification accuracy. we also attempt to find the optimum feature set by training the SVM model using various combinations of features. The results for this test show that the highest classification accuracy and precision values are 97.48% and 96.91% respectively, using the average power from 1-8 Hz in 1 Hz bin resolution as features. The proposed feature set achieves an accuracy and precision of 97.94% and 98.73% respectively, while incurring lower training error. This suggests that the proposed feature selection scheme is optimal for EEG drowsiness detection using SVM.

In order to account for the ambiguity in defining drowsiness with respect to the five stages of sleep we combined sleep stages 1 and 2, thereby including both possible definitions of drowsiness. Using the optimum feature set established previously we were able to achieve an accuracy and precision of 98.2% and 97.88%, respectively. Clearly, these results demonstrate that we can effectively distinguish between awake and all possible drowsy states with great confidence. Finally, we provide a comparison of our drowsiness classification method against prior work by Park, Lin, Picot, and Yeo et al [9], [11], [12], [17]. We find that not only is our method superior to threshold based methods in terms of performance and accuracy, but also better than SVM based models based on traditional EEG frequency broadbands in terms of flexibility and feasibility.

Our research presented in this thesis shows that subbanding is crucial in analyzing complex frequency components of EEG waveforms. Subbanding allows for fine control of feature selection and reduces the risk of masking behavior prevalent in traditional EEG frequency bands. It also enables the use of various methods to account for interpersonal variability between different people, a feat not easily accomplished using traditional EEG bands.

REFERENCES

1. R. Broughton and J. Hasan. Quantitative topographic electroencephalographic mapping during drowsiness and sleep onset. Journal of Clinical Neurophysiology, 12(4):372–386, 1995.

2. J. L. Cantero, M. Atienza, and R. M. Salas. Human alpha oscillations in wakefulness, drowsiness period, and rem sleep: different electroencephalographic phenomena within the alpha band. Neurophysiologie Clinique/Clinical Neurophysiology, 32(1):54–71, 2002. Copyright © 2002 Elsevier Masson SAS. All rights reserved.

3. C. Cortes and V. Vapnik. Support-vector networks. Machine Learning, 20(3):273–297, 1995.

4. L. De Gennaro, M. Ferrara, and M. Bertini. The boundary between wakefulness and sleep: quantitative electroencephalographic changes during the sleep onset period. Neuroscience, 107(1):1–11, 2001.

5. A. Gevins, G. Zeitlin, S. Ancoli, and C. Yeager. Computer rejection of eeg artifact. ii. contamination by drowsiness. Electroencephalography and Clinical Neurophysiology, 43(1):31–42, 1977.

6. A. L. Goldberger, L. A. N. Amaral, L. Glass, J. M. Hausdorff, P. C. Ivanov, R. G. Mark, J. E. Mietus, G. B. Moody, C.-K. Peng, and H. E. Stanley. PhysioBank, PhysioToolkit, and PhysioNet: Components of a new research resource for complex physiologic signals. Circulation, 101(23):e215–e220, 2000 (June 13). Circulation Electronic Pages: http://circ.ahajournals.org/cgi/content/full/101/23/e215 PMID:1085218; doi: 10.1161/01.CIR.101.23.e215.

7. T. Joachims. SVM light, http://svmlight.joachims.org, 2002. Accessed Nov. 2012

8. W. Klimesch. Eeg alpha and theta oscillations reflect cognitive and memory performance: a review and analysis. Brain Research Reviews, 29(2):169–195, 1999.

9. C.-T. Lin, C.-J. Chang, B.-S. Lin, S.-H. Hung, C.-F. Chao, and I.-J. Wang. A real-time wireless brain–computer interface system for drowsiness detection. Biomedical Circuits and Systems, IEEE Transactions on, 4(4):214–222, 2010.

10. J. M. Lyznicki, T. C. Doege, R. M. Davis, M. A. Williams, et al. Sleepiness, driving, and motor vehicle crashes. JAMA: the Journal of the American Medical Association, 279(23):1908–1913, 1998.

11. J. Park, L. Xu, V. Sridhar, M. Chi, and G. Cauwenberghs. Wireless dry eeg for drowsiness detection. In Engineering in Medicine and Biology Society, EMBC, 2011 Annual International Conference of the IEEE, pages 3298–3301. IEEE, 2011.

12. A. Picot, S. Charbonnier, and A. Caplier. On-line detection of drowsiness using brain and visual information. Systems, Man and Cybernetics, Part A: Systems and Humans, IEEE Transactions on, 42(3):764–775, 2012.

13. Kales, Anthony. and Rechtschaffen, Allan. and University of California, Los Angeles. Brain Information Service. and NINDB Neurological Information Network (U.S.). A manual of standardized terminology, techniques and scoring system for sleep stages of human subjects. Allan Rechtschaffen and Anthony Kales, editors U. S. National Institute of Neurological Diseases and Blindness, Neurological Information Network Bethesda, Md 1968.

14. M. G. Terzano, L. Parrino, A. Sherieri, R. Chervin, S. Chokroverty, C. Guilleminault, M. Hirshkowitz, M. Mahowald, H. Moldofsky, A. Rosa, et al. Atlas, rules, and recording techniques for the scoring of cyclic alternating pattern (cap) in human sleep. Sleep Medicine, 2(6):537–553, 2001.

15. Vapnik, Vladimir Naumovich. Statistical Learning Theory. New York: Wiley, 1998. Print.

16. K. P. Wright Jr, P. Badia, A. Wauquier, et al. Topographical and temporal patterns of brain activity during the transition from wakefulness to sleep. Sleep, 18(10):880, 1995.

17. M. V. Yeo, X. Li, K. Shen, and E. P. Wilder-Smith. Can svm be used for automatic eeg detection of drowsiness during car driving? Safety Science, 47(1):115–124, 2009. Copyright (2009), with permission from Elsevier.

18. Jasper, Herbert Henri. The ten twenty electrode system of the international federation. Electroencephalography and Clinical Neurophysiology 10 (1958): 371-375.

19. Shaoda Yu, Peng Li, Honghuang Lin, Rohani, E., Gwan Choi, Botang Shao, Qian Wang, "Support Vector Machine Based Detection of Drowsiness Using Minimum EEG Features", Social Computing (SocialCom), 2013 International Conference on Social Computing, 827-835, 8-14 Sept. 2013.

20. Loomis AL, Harvey EN, Hobart GA., III Cerebral states during sleep, as studied by human brain potentials. J Exp Psychol. 1937;21:127–44.

21. Dement, William, and Nathaniel Kleitman. The relation of eye movements during sleep to dream activity: an objective method for the study of dreaming. Journal of Experimental Psychology 53.5 (1957): 339.

22. Elsevier. Report of the committee on methods of clinical examination in electroencephalography: 1957, Electroencephalography and Clinical Neurophysiology 2(10): 370–375, 1958 Copyright (1958), with permission from Elsevier.

23. José Luis Cantero, Mercedes Atienza, Rosa M Salas, State-modulation of cortico-cortical connections underlying normal EEG alpha variants, Physiology & Behavior, 71/1–2, 107–115, Copyright (2000), with permission from Elsevier.